ELSEVIER

Contents lists available at ScienceDirect

# Palaeogeography, Palaeoclimatology, Palaeoecology

journal homepage: www.elsevier.com/locate/palaeo





# Enigmatic carbonate isotope values in shark teeth: Evidence for environmental and dietary controls

Molly E. Karnes <sup>a,b,\*</sup>, Rachel L. Chan <sup>a</sup>, Jonathon P. Kuntz <sup>a</sup>, Michael L. Griffiths <sup>c</sup>, Kenshu Shimada <sup>d,e,f</sup>, Martin A. Becker <sup>c</sup>, Harry M. Maisch IV <sup>g</sup>, Robert A. Eagle <sup>h</sup>, Joan Brenner-Coltrain <sup>i</sup>, Shawn Miller <sup>j</sup>, Sora L. Kim <sup>a</sup>

- <sup>a</sup> Department of Life and Environmental Sciences, University of California, Merced, 5200 Lake Rd, Merced, CA 95343, United States of America
- b Department of Earth and Atmospheric Sciences, Indiana University, 702 N. Walnut Grove Ave, Bloomington, IN 47405, United States of America
- <sup>c</sup> Department of Environmental Science, William Paterson University, 300 Pompton Rd, Wayne, NJ 07470, United States of America
- d Department of Environmental Science and Studies, DePaul University, 1110 W Belden Ave, IL 60614, United States of America
- e Department of Department of Biological Sciences, DePaul University, 2325 N Clifton Ave, Chicago, IL 60614, United States of America
- f Sternberg Museum of Natural History, 3000 Sternberg Dr, Hays, Kansas 67601, United States of America
- g Department of Marine and Earth Sciences, Florida Gulf Coast University, 10501 FGCU Blvd S, Fort Myers, FL 33965, United States of America
- h Institute of the Environment and Sustainability, Department of Atmospheric and Oceanic Sciences, University of California, Los Angeles, 520 Portola Plaza, Los Angeles, CA 90095, United States of America
- Department of Anthropology, University of Utah, 260 Central Campus Dr, Salt Lake City, UT 84112, United States of America
- <sup>j</sup> School of Biological Sciences, University of Utah, 201 Presidents' Cir, Salt Lake City, UT 84112, United States of America

#### ARTICLE INFO

Editor: M Zhao

Keywords: Stable isotope Carbon Oxygen Phosphate Enameloid Extant

# ABSTRACT

Shark teeth are abundant in the fossil record and integrate physiological information, ecological interactions, and paleo-oceanographic conditions in their chemistry. Fossil shark teeth are well suited for stable isotope analysis because their enameloid is resistant to diagenetic alteration due to its high chemical stability. Although often used in paleoecological studies of mammals, carbonate carbon isotope compositions ( $\delta^{13}C_{CO3}$ ) in shark enameloid have remained enigmatic. Here, we investigate multiple stable isotope systems ( $\delta^{13}C_{org}$ ,  $\delta^{13}C_{CO3}$ ,  $\delta^{18}O_{CO3}$ ,  $\delta^{18}O_{PO4}$ ) within modern shark teeth to determine relationships between the different systems and build an interpretative framework for future studies of both modern and fossil sharks. There is a weaker than expected correlation between  $\delta^{18}O_{PO4}$  and  $\delta^{18}O_{CO3}$  values in modern shark teeth ( $r^2=0.44$ ), which contrasts with mammalian studies to date and suggests this metric is not an appropriate test for diagenetic alteration in fossil shark teeth. Organic carbon isotope composition ( $\delta^{13}C_{org}$ ) measured from modern dental collagen ranges from -16.0% to -10.8%. The enameloid  $\delta^{13}\hat{C}_{CO3}$  values we measured are much higher than collagen, ranging from -6.0% to 10.3%, and there is no direct relationship between  $\delta^{13}C_{OP}$  and  $\delta^{13}C_{CO3}$  values in shark teeth. Instead, we found the fractionation ( $\epsilon$ ) between  $\delta^{13}C_{org}$  and  $\delta^{13}C_{CO3}$  values to correspond with  $\delta^{18}O_{CO3}$  values but not  $\delta^{18}O_{PO4}$  values. This could be due to the carbon source in shark enameloid being partitioned between dietary carbon and dissolved inorganic carbon (DIC) or physiological differences in the tooth formation process changing the fractionation of carbonate isotopes. We applied the fractionation factor from modern teeth to carbonate isotope compositions of fossil shark teeth to predict  $\delta^{13}C_{org}$  values. Although the carbon sources to shark enameloid carbonate needs further investigation, our results suggest that fossil shark teeth could provide insights into carbon cycling of ancient marine ecosystems.

### 1. Introduction

Sharks have a rich and abundant fossil record, documenting their

persistence through multiple mass extinctions and climate events since their origination (Maisey, 2012), but many aspects of their ecology remain elusive. Past studies on shark paleoecology gleaned insights

E-mail address: mokarnes@iu.edu (M.E. Karnes).

https://doi.org/10.1016/j.palaeo.2023.111943

<sup>\*</sup> Corresponding author at: Department of Life and Environmental Sciences, University of California, Merced, 5200 Lake Rd, Merced, CA 95343, United States of America.

based on sedimentology and stratigraphy, community assembly, and relative abundance. Recent paleobiological studies are increasingly using quantitative approaches (Whitenack et al., 2022), such as stable isotope analysis (SIA). The SIA of fossil shark teeth has been primarily used for Cenozoic paleo-oceanographic reconstructions with respect to salinity and temperature gradients associated with tectonics, upwelling, and currents (e.g., Amiot et al., 2008; Kiel et al., 2023; Kim et al., 2014, 2020; Kocsis et al., 2007, 2008; Lécuyer et al., 1996; Vennemann et al., 2001; Vennemann and Hegner, 1998).

There is growing interest in using SIA to probe shark paleoecology (Kast et al., 2022; Kim et al., 2020; McCormack et al., 2022). Stable isotope analysis is a commonly used tool in both modern and paleoecological studies to answer questions about diet and food web structure, including changes through ontogeny and migration (Shiffman et al., 2020). Most neontological (modern) studies of sharks focus on soft tissues or collagen extracted from dentin to discern facets of foraging ecology (Polo-Silva et al., 2012; Shipley et al., 2021; Zeichner et al., 2017). However, the fossil record for sharks is primarily comprised of teeth, as their cartilaginous skeletons are rarely preserved. The mineralized outer portion of shark teeth, known as enameloid, is composed of a biological fluorapatite making it ideal for SIA in fossils because it is highly resistant to chemical alteration (Vennemann et al., 2001; Enax et al., 2012). Investigating the enameloid of modern shark teeth with a suite of stable isotope systems will help bridge our knowledge of modern and paleo shark ecology.

To investigate isotopic relationships and create a modern interpretive framework for shark teeth, we compiled an array of modern shark

teeth and analyzed the stable isotope composition of the following systems: phosphate oxygen  $(\delta^{18}O_{PO4})$ , carbonate oxygen  $(\delta^{18}O_{CO3})$ , carbonate carbon  $(\delta^{13}C_{CO3})$ , and organic carbon  $(\delta^{13}C_{org})$ . We find limited correlation between  $\delta^{18}O_{PO4}$  and  $\delta^{18}O_{CO3}$  values as well as  $\delta^{13}C_{CO3}$  and  $\delta^{13}C_{org}$  values, but propose an explanation based on the correlation of  $\delta^{18}O_{CO3}$  values to carbon enrichment values. Then, we use this relationship to estimate  $\delta^{13}C_{org}$  values of fossil shark teeth. Future paleoecological studies will benefit from an interpretive framework for stable isotope geochemistry established in modern shark teeth.

## 1.1. Tooth organization, structure, and composition

Sharks have a polyphyodont dentition and a unique process of tooth replacement that resembles a conveyor belt (Fig. 1A,B; Smith et al., 2012; Berkovitz and Shellis, 2017). Teeth are organized into rows oriented along the jaw (Fig. 1A) with files perpendicular to the jaw at different stages of development (Fig. 1B). Teeth at the buccal edge of the jaw are the oldest row of teeth and are referred to as "functional teeth" (Fig. 1B). Functional teeth are shed and replaced every few weeks depending on the species (Berkovitz and Shellis, 2017). This continuous tooth replacement occurs throughout an individual shark's lifetime and produces the abundant and prolific fossil record for sharks.

Shark teeth are composed of a central dentin region covered by a 0.2–0.9 mm layer of enameloid that is thickest at the tip and thins towards the root (Fig. 1C; Vennemann et al., 2001). Mineralogically, enameloid is a fluoride-rich biogenic apatite primarily composed of fluorapatite ( $Ca_5(PO_4)_3F$ ) with occasional substitutions of hydroxide for

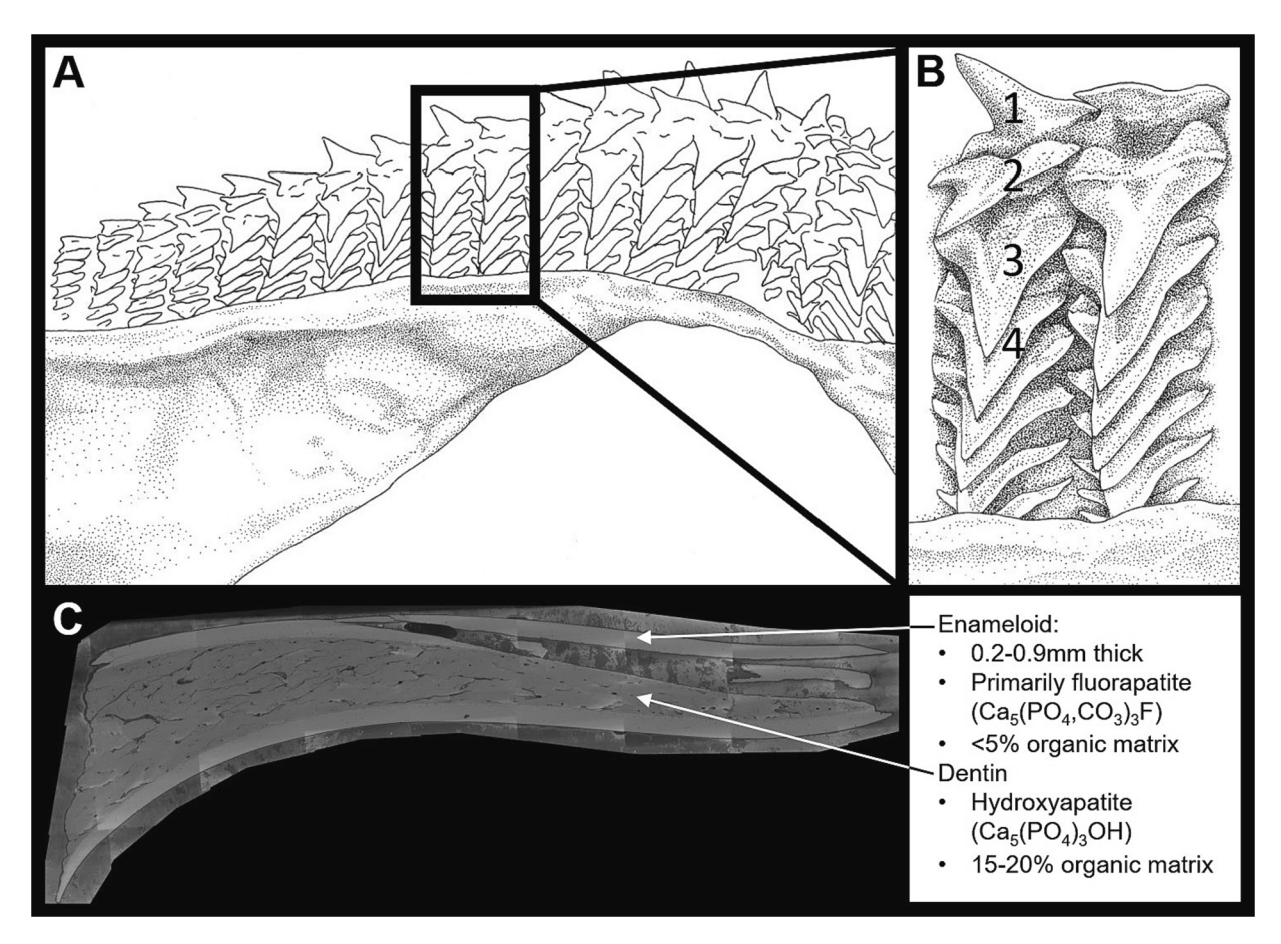


Fig. 1. A: Sketch of a shark jaw and teeth (*Sphyrna mokarran*, great hammerhead shark) showing the arrangement of teeth within a jaw (rows are parallel and files are perpendicular to the jaw). B: A close-up view showing two series of teeth, where teeth are numbered from the buccal edge of the jaw with 1 being the oldest tooth in the file (sketches by Sarah Baird). C: SEM cross-section image of a modern shark tooth (*Carcharias taurus*, sand tiger shark), showing the regions of enameloid and dentin (image generated by James Schiffbauer at the University of Missouri X-ray microanalysis lab (MizzouμX); the tooth is embedded in resin, as the tip of the tooth is fractured).

fluoride ( $Ca_5(PO_4)_3OH$ , hydroxyapatite) and carbonate for phosphate ( $Ca_5(PO_4,CO_3)_3F$ , carbonated apatite) (Miake et al., 1991; Moeller et al., 1975; Suga et al., 1991) with ~2 wt% carbonate (Vennemann et al., 2001). The high fluoride concentration (3.3 wt%, Glas, 1962) and low organic content (<5%, Sire et al., 2007) in enameloid make it more resistant to diagenetic alteration than dentin (Hättig et al., 2019) which has a much higher organic content (15–20%, Enax et al., 2012).

Enameloid performs the same function as mammalian enamel but differs in the origin of formation. In mammalian teeth, dentine is produced first by mesenchymal odontoblasts, followed by the production of enamel by ameloblasts in the inner dental epithelium (IDE). In sharks, this order is reversed and the enameloid production occurs in between the IDE and the ectomesenchymal cells of the dental papilla by both ameloblasts and odontoblasts (Berkovitz and Shellis, 2017; Fellah et al., 2021; Francillon-Vieillot et al., 1990; Gillis and Donoghue, 2007). The shark "tooth conveyor belt" occurs within the dental lamina, a flat layer of epithelial tissue parallel to the jaw. Teeth move forward through the dental lamina as they mature until they erupt and eventually become functional teeth; depending on the species, there are varying number of erupted teeth in functional positions (Jambura et al., 2018, 2019; Berkovitz and Shellis, 2017). During the enamel maturation process in mammals the enzymes enamelysin (MMP-20) and kallikrein 4 (KLK4) aid in the degradation and removal of the organic matrix that scaffolds the development of the tooth (Lu et al., 2008) and aids in the growth of large, well mineralized crystals in the presence of zinc (Goettig et al., 2010; Kocsis et al., 2015). Because of the high zinc concentrations reported in shark enameloid, especially near the highly mineralized cutting edges, it's hypothesized that these enzymes also play a role in enameloid mineralization (Kocsis et al., 2015; Leuzinger et al., 2023). Most stable isotope studies examining tooth formation processes feature mammals (e.g., Blumenthal et al., 2014; Green et al., 2017; Passey and Cerling, 2002) but this discrepancy in enamel and enameloid formation may be the cause of differences in carbonate sources.

# 1.2. Enigmas of oxygen and carbon stable isotope composition in shark teeth

Oxygen isotope compositions of teeth vary based on the  $\delta^{18}$ O value of the organism's body water and temperature at time of formation (Kohn and Cerling, 2002; Kolodny et al., 1983; Lécuyer et al., 2013; Pucéat et al., 2010). Most sharks are ectotherms; therefore, their body temperature reflects environmental temperature. Furthermore, as aquatic ectotherms, it is assumed their body water is in steady state with environmental water. With independent proxy data for seawater  $\delta^{18}$ O values, studies can use fossil shark teeth as regional or nearshore paleothermometers (Chan, 2022; Zacke et al., 2009). Conversely, in systems where independent temperature estimates are available,  $\delta^{18}$ O values of bioapatite can help constrain water salinity or isotope composition (Kim et al., 2014; Waddell and Moore, 2008; Kocsis et al., 2007). In biogenic phosphates like enameloid,  $\delta^{18}$ O values can be measured in both phosphate and carbonate. It is assumed that as the tooth forms, both phosphate and carbonate use body water as a substrate and therefore the offset between their  $\delta^{18}$ O values should be constant (Kohn and Cerling, 2002). Based on mammal studies, an expected carbonate-phosphate oxygen isotope offset of ~9% is often used to assess diagenetic alteration in fossil specimens (Bryant et al., 1996; Eagle et al., 2011; Iacumin et al., 1996; Kohn and Cerling, 2002; Martin et al., 2008; Zazzo et al., 2004b). However, a large and inconsistent offset is reported in sharks (6.0-11.8%; Vennemann et al., 2001), suggesting that earlier assumptions about the relationship between carbonate and phosphate oxygen isotope composition may not hold true for sharks.

Carbon isotopes can be measured in both organic and inorganic materials. Organic carbon isotope values ( $\delta^{13}C_{org}$ ) are incorporated into consumer tissues via diet, tracing energy flow through a food web with an average fractionation of ~1‰ between trophic levels (DeNiro and Epstein, 1978). The ecosystem isotopic baseline is set by primary

producers and in marine systems represents the availability of fresh CO<sub>2</sub> sources for photosynthesis and the organisms' ability to fully express isotopic discrimination (Casey and Post, 2011). Inorganic carbon isotope values in most bioapatite ( $\delta^{13}C_{CO3}$ ) are related to  $\delta^{13}C_{org}$  through respiration. Respired metabolic CO<sub>2</sub> in blood is in isotopic equilibrium with enamel at time of formation (Passey et al., 2005). The  $\delta^{13}C_{CO3}$ values are thought to incorporate aspects of diet based on studies with mammals (Cerling and Harris, 1999; Passey et al., 2005) and have a close linear relationship with  $\delta^{13}C_{org}$  (Codron et al., 2018); however this framework is not valid for sharks. Previously reported results of enameloid  $\delta^{13}C_{CO3}$  and whole tooth (enameloid + dentine)  $\delta^{13}C_{CO3}$  found consistent <sup>13</sup>C enrichment in enameloid (Vennemann et al., 2001). Preliminary data from modern shark teeth lack the linear relationship between  $\delta^{13}C_{CO3}$  and  $\delta^{13}C_{org}$  values seen in mammals (e.g., Cerling and Harris, 1999; Passey et al., 2005). Previous studies have also noted the enigmatic  $\delta^{13}C_{CO3}$  values in fossil shark teeth (Kocsis et al., 2014; Ounis et al., 2008; Van Baal et al., 2013).

In some marine organisms,  $\delta^{13}C_{CO3}$  values in biomineralized substrate record a more complicated signal that confounds diet and environmental inputs. For example,  $\delta^{13}C_{CO3}$  values in fish otoliths are a combined signal from respiration and dissolved inorganic carbon (DIC) in seawater, with the relative proportions controlled by metabolism (Chung et al., 2019). We hypothesize that similar processes of DIC incorporation during enameloid maturation or after tooth eruption may affect both carbonate carbon and oxygen isotope compositions of shark enameloid. Alternatively, carbonate carbon isotopic compositions may be affected by isotopic fractionation during mineralization. The enzymatic process (described in §1.1) paired with sharks' faster rate of tooth growth and replacement may selectively remove <sup>12</sup>C that would result in <sup>13</sup>C-enrichment of the remaining carbon pool during mineralization (Leuzinger et al., 2023). In addition to the relationship between organic and inorganic  $\delta^{13}C$  values, the differentiation between carbonate and phosphate oxygen isotope values ( $\delta^{18}O_{CO3}$  and  $\delta^{18}O_{PO4}$ ) warrants further investigation. Previous findings determined a large variation in  $\delta^{18}O$  offset and a wider range of  $\delta^{18}O_{CO3}$  values compared to  $\delta^{18}O_{PO4}$ values, which suggests that there is an unknown factor in biomineralization affecting isotopic composition of carbonate but not phosphate (Vennemann et al., 2001).

# 2. Materials and methods

# 2.1. Sample collection

Powdered enameloid samples were collected, then powdered dentin samples were separately collected from 153 modern shark teeth, including wild and aquarium kept individuals, some of which were part of a previously published captive feeding study (Kim et al., 2012a, 2012b). Twenty-eight samples from the New York Aquarium have  $\delta^{18}\mathrm{O}_{PO4}$  values previously published in Griffiths et al. (2023). The Sphyrna zygaena (smooth hammerhead shark) teeth were extracted from a formalin-preserved specimen from the University of Utah collections. This dataset includes individuals from nine families (Carcharhinidae, Carchariidae, Lamnidae, Megachasmidae, Odontaspididae, Somniosidae, Sphyrnidae, Squalidae, and Triakidae; species and localities in Table 1). For modern samples enameloid was analyzed for  $\delta^{18}\mathrm{O}_{PO4}$ ,  $\delta^{13}\mathrm{C}_{CO3}$ , and  $\delta^{18}\mathrm{O}_{CO3}$ ; and dentin was analyzed for  $\delta^{13}\mathrm{C}_{org}$  and  $\delta^{15}\mathrm{N}_{org}$ .

Powdered enameloid samples were also collected from 54 fossil shark teeth that range from Cretaceous to Pliocene in age and include six families (Anacoracidae, Carcharhinidae, Lamnidae, Mitsukurinidae, Odontaspididae, and Otodontidae; two samples from an uncertain family (*Parotodus benedinii*); Table 2). Although not used in this study, it is worth noting that  $\delta^{18}\mathrm{O}_{PO4}$  values for some of the Miocene and Pliocene specimens are previously published in Griffiths et al. (2023) to investigate endothermy in *Otodus megalodon* (indicated in Table 2); this study publishes new carbonate isotope results from these specimens. In addition to the fossil specimens sampled in this study, we also included

Table 1 The locality, species, and number of all modern teeth included in this study.

Specimens with phosphate results published in Griffiths et al. (2023) are indicated with '; carbonate results for these specimens were generated as part of this

Modern Teeth Loca	alities and Species	
Location	Species	n
California, USA	Lamna ditropis	3
	Sphyrna zygaena	8
Santa Cruz, California, USA (captive)	Triakis semifasciata	7
Delaware Bay, USA	Carcharias taurus	39
Florida, USA	Carcharhinus limbatus	5
Hawaii, USA	Megachasma pelagios	1
	Odontaspis ferox	3
New York Aquarium, USA (captive)	Carcharias taurus^	15
	Carcharhinus plumbeus^	15
	Sphyrna zygaena	5
	Carcharhinus brevipinna	1
Japan	Mustelus manazo	1
	Centrophorus acus	6
	Centroscymnus owstonii	1
	Sphyrna mokarran	4
	Carcharodon carcharias	6
South Africa	Sphyrna mokarran 4 Carcharodon carcharias 6 Carcharhinus leucas 19	
	Carcharhinus obscurus	nus obscurus 5
	Galeocerdo cuvier	9

previously published enameloid carbonate data ( $\delta^{13}C_{CO3}$  and  $\delta^{18}O_{CO3}$ ) compiled from six studies (Aguilera et al., 2017; Kim et al., 2014; Kocsis et al., 2014; Kolodny and Luz, 1992; Ounis et al., 2008; Van Baal et al., 2013). All fossil carbonate data were included in our estimates of organic carbon values ( $\delta^{13}C_{org}^{*}$ ). Localities, age, species, and number of all fossils sampled for this study are included in Table 2. Modern and fossil specimens are catalogued at museums and specimen identification numbers are included in the supplemental data table.

# 2.2. Enameloid - pre-treatment

For the analysis of enameloid, 4-5 mg of sample were collected from all shark teeth using a Dremel on low speed with a 300-um diamond tipped bit. These samples were then treated with 2.5% NaOCl overnight to remove organic contaminants, rinsed five times with deionized water and dried overnight in an oven at  $\sim$ 50 °C. Modern samples were then split into two portions for carbonate and phosphate preparation.

Fossil samples need an additional treatment of acetic acid to remove potential secondary carbonates before subsequent chemistry was performed (Trueman et al., 2004). Once samples had been rinsed of NaOCl, 0.5 mL 1 M acetic acid buffered to pH  $\sim 5 \text{ with } 0.91 \text{ M}$  calcium acetate was added. Samples were allowed to react in the refrigerator for 24 h. After reaction, samples were rinsed five times with deionized water and dried overnight in an oven at ~50 °C.

# 2.3. Enameloid – carbonate $\delta^{13}C$ and $\delta^{18}O$ values

For carbonate analysis, a subsample of enameloid powder as described in  $\S 2.2$  was weighed to  $\sim 0.5$  mg into glass exetainers (3.7 mL round bottom vial, Labco). The headspace of the vials was flushed with He gas. Samples were heated to 70  $^{\circ}$ C and  $\sim 0.1 \,\mu\text{L}$  of 104% phosphoric acid was added and allowed to digest fully (~2 h). This reaction produces  $CO_2$ , which was measured for  $\delta^{13}C$  and  $\delta^{18}O$  values using a Gas-Bench coupled to a Delta V Plus continuous flow isotope ratio mass spectrometer (cf-irms) with a Conflo IV at the Stable Isotope Ecosystem Lab of the University of California Merced (SIELO). We determined  $\delta^{13}$ C and  $\delta^{18}O$  relative to Vienna Pee Dee Belemnites (VPDB). Data were corrected for linearity and drift using a suite of calibrated reference materials (Carrara Marble [n = 28], NBS 18 [n = 31], USGS 44 [n =30]). Long-term standard deviation for the instrument is  $\pm 0.2\%$  for both  $\delta^{13}$ C and  $\delta^{18}$ O values.

Table 2 The locality, geologic age, species, and number of all fossil teeth analyzed in this

study. Although not reported here, specimens with phosphate results published in Griffiths et al. (2023) are indicated with '; carbonate results for these specimens were generated as part of this study.

	Fossil Teeth Lo	calities and Spe	cies	
Location	Stratigraphy Lisbon-Tallahatta	Period	Species Striatolamia	r
	Formation	Eocene	macrota Scapanorhynchus	1
Alabama, USA	Eutaw Formation Arkadelphia	Cretaceous	texanus Carcharias	1
Arkansas, USA	Formation	Cretaceous	holmdelensis Carcharodon	1
			hastalis^	1
			Isurus planus^	
	Sharktooth Hill		Physogaleus sp.^	
	Bonebed	Miocene	Carcharhinus sp.^ Carcharodon	
			carcharias^	
	San Mateo		Otodus megalodon^	:
California, USA	Formation	Pliocene	Carcharhinus sp.	
Florida, USA	Peace River Formation	Miocene- Pliocene	Otodus megalodon	
			Carcharias sp.^	:
	Pungo River		Carcharias taurus^	
	Formation	Miocene	Carcharodon hastalis^	
			Otodus chubutensis^	:
			Carcharias taurus^	
North Carolina, USA			Carcharodon carcharias^	:
	Yorktown		Carcharodon	
	Formation	Pliocene	hastalis^	
			Isurus oxyrinchus	:
			Otodus megalodon^	(
			Parotodus benedinii^	
New Jersey,	Shark River		Carcharhinus sp.^ Striatolamia	
USA	Formation	Eocene	macrota	
South Carolina,	Ten Mile Hill	Locciic	Carcharodon	
USA	Formation	Pliocene	hastalis	:
N. Banks Island,			Striatolamia	
Canada	Eureka Sound	Eocene	macrota	2
France	Componion		Scapanorhynchus	
	Campanian deposit	Cretaceous	sp.	
	•		Squalicorax kaupi	
Kuzubukuro,	Iwadono	Miocene	Otodus megalodon	
Japan	Formation	mocenc	Parotodus benedini	
Choshi City,	Na-arai		Carcharodon	
Japan	Formation	Pliocene	carcharias^	
•	Middle Eocene		Otodus megalodon^	
Kazakhstan	deposit	Eocene	Otodus sokolovi	
Morocco	Early Eocene	Eocene	Striatolamia	
	deposit	Locuit	macrota	

The S. zygaena samples from the University of Utah collections were weighed to ~0.25 mg into glass exetainers that were then flushed with He gas. Samples underwent acid digestion via phosphoric acid. The resulting  $CO_2$  was measured for  $\delta^{13}C$  and  $\delta^{18}O$  values on a Thermo Finnigan Gas Bench II connected to a cf-irms Thermo Finnigan MAT 253 via Conflo IV at the Stable Isotope Ratio Facility for Environmental Research (SIRFER) at the University of Utah. All data were corrected using a suite of calibrated reference materials (LSVEC [n = 4] as well as Carrara [n = 4] and Marble [n = 3], both internal lab standards are calibrated against international reference materials). Long-term standard deviation for the instrument is  $\pm 0.2\%$  for both  $\delta^{13}C$  and  $\delta^{18}O$ values.

# 2.4. Enameloid – phosphate $\delta^{18}$ O values

For phosphate oxygen isotope analysis, a subsample of enameloid

powder as described in §2.2 was used to precipitate silver phosphate using the "rapid" precipitation method from Mine et al. (2017). First, 1.5 mg of sample were dissolved in 50 μL 2 M HNO<sub>3</sub> overnight. The next day, CaF2 was precipitated using 30  $\mu$ L 2.9 M HF and 50  $\mu$ L 2 M NaOH and the supernatant was transferred to a new microcentrifuge tube. The  $CaF_2$  pellet was rinsed with 50  $\mu L$  0.1 M NaF and this supernatant was also transferred to the new tube. Silver phosphate was precipitated from the supernatant by adding 180 µL of a silver ammine solution (0.37 M AgNO<sub>3</sub>, 1.09 M NH<sub>4</sub>OH). The pH was adjusted to 6–7 with <10uL dilute HNO<sub>3</sub> or NH<sub>4</sub>OH for optimal precipitation (additional discussion of this pH adjustment detailed in Mine et al. (2017)). Silver phosphate crystals were rinsed five times with deionized water and dried overnight at 50 °C. All phosphate samples were weighed in triplicate to 0.15–0.20 mg in silver capsules and measured for  $\delta^{18}$ O values using a TC/EA coupled to a Delta V Plus cf-irms with a Conflo IV at the SIELO. We determined δ<sup>18</sup>O relative to Vienna Standard Mean Ocean Water (VSMOW). All data were corrected for linearity and drift using a suite of calibrated reference materials (USGS 80 [n = 95], USGS 81a [n = 91], IAEA 601 [n = 52]). Long-term standard deviation for the instrument is  $\pm 0.4\%$  for  $\delta$  <sup>18</sup>O.

# 2.5. Dentin – organic $\delta^{13}C$ values

To determine the stable isotope composition of organic carbon ( $\delta^{13}C_{org}$ ), collagen was isolated from tooth dentin. Powdered dentin samples were collected from all modern shark teeth using a Dremel on low speed with a 300- $\mu$ m diamond tipped bit. These samples were then demineralized using chilled 0.1 M HCl following Trayler et al., 2023. After demineralization, samples were rinsed five times with deionized water and freeze dried overnight. Samples were weighed to 0.4–0.5 mg in tin capsules. Collagen samples were measured using a Costech 4010 Elemental Analyzer coupled to a Delta V Plus cf-irms with a Conflo IV at the SIELO. All data were corrected for linearity and drift using a suite of calibrated reference materials (USGS 40 [n=36], USGS 41a [n=23], costech acetanilide [n=35]). Long-term standard deviation for the instrument is  $\pm 0.1\%$  for  $\delta^{13}$ C and  $\pm 0.2\%$  for  $\delta^{15}$ N values.

For the S. zygaena specimens from the University of Utah collections, a whole tooth was demineralized in 0.6 N HCl at 4 °C. The supernatant was decanted and replaced daily until complete (supernatant free of Ca<sub>3</sub>(PO<sub>4</sub>)<sub>2</sub>), no visible density gradient, and sample "spongy" when probed). The sample was then rinsed to neutrality and soaked in 5% KOH. The KOH was poured off and replaced daily for removal of organic contaminants. After acid and base extraction, the sample was rinsed to neutrality again and gelatinized in 5 mL of water (pH 3) for 24 h at 90 °C. Water-soluble and insoluble phases were then separated by filtration with a 0.45 µm, Luer-Lok syringe filter and the water-soluble phase was lyophilized and weighed to obtain a final collagen yield. Collagen samples were measured for  $\delta^{13}$ C values by flash combustion on a cf-irms coupled to elemental analyzer at SIRFER. All data were corrected for linearity and drift using a suite of calibrated reference materials (UU-CN-1 [n = 3], UU-CN-2 [n = 3], both internal lab standards are glutamic acids calibrated against USGS 40 and USGS 41). Long-term standard deviation for the instrument is  $\pm 0.2\%$  for  $\delta^{13}\text{C}$  values.

# 2.6. Estimating organic carbon ( $\delta^{13}C$ )

We compared the offset between the two  $\delta^{13}C$  values ( $\delta^{13}C_{CO3}$  and  $\delta^{13}C_{org}$ ), based on the fractionation ( $\epsilon$ ) defined as:

$$lpha = \left( \frac{(1000 + \delta^{13} C_{CO3})}{(1000 + \delta^{13} C_{org})} \right)$$

 $\varepsilon = 1000*ln(\alpha).$ 

This calculation of fractionation was chosen over the simpler  $\Delta_{A-B} = \delta_{A^-} \delta_B$  because  $\Delta_{A-B}$  is only a good approximation of fractionation when values are <10% (Sharp, 2017). Additionally, we refer to  $\epsilon^*$  given that

this value is for a biological and non-reversible reaction (Cerling and Harris, 1999). We used only functional teeth (position 1, Fig. 1) for the regression as the carbon offset varies between teeth in different positions, possibly due to changing CO<sub>3</sub> concentration during enameloid maturation (Supplemental Fig. 1).

In addition, we attempted to determine the proportional inputs of organic and inorganic carbon sources to enameloid ( $\delta^{13}C_{CO3}$ ) with a simple two-component mixing model. The two-component model was adapted from Chung et al. (2019) to incorporate two  $\epsilon$  to account for offset from dietary carbon (org) and DIC sources:

$$\delta^{13}C_{CO3} = (1 - x)(\delta^{13}C_{org} + \varepsilon_{org}) + x(\delta^{13}C_{DIC} + \varepsilon_{DIC})$$

where x is the proportion input of DIC and  $\delta^{13}C_{DIC}=1.252$ , (Tagliabue and Bopp, 2008). We used results from all extant shark  $\delta^{13}C_{CO3}$  and  $\delta^{13}C_{org}$  values in this study, substituted  $\epsilon_{org}$  and  $\epsilon_{DIC}$  from -30 to 30, and constrained x between 0 and 1 since it is a proportion input. All model code is available in supplemental material.

#### 2.7. Statistical analysis

All statistical analyses were done in R (2023, v 4.3.1). Pearson's correlation coefficient (r) was calculated using the function "cor.test" to measure the strength of correlation between continuous variables ( $\delta^{18}O_{PO4}$  vs.  $\delta^{18}O_{CO3}$ ,  $\delta^{13}C_{org}$  vs.  $\delta^{13}C_{CO3}$ , and  $\delta^{13}C_{CO3}$  vs.  $\delta^{18}O_{CO3}$ ). For  $\epsilon^*$  vs.  $\delta^{18}O_{CO3}$  and  $\epsilon$  vs.  $\delta^{18}O_{PO4}$  we applied linear regression models using the function "lm". We report the test used, test statistic, and significance (where relevant) in the results text.

#### 3. Results

#### 3.1. Modern oxygen isotope compositions

We used a single tooth from 117 modern specimens to generate carbonate and phosphate  $\delta^{18}O$  values. We generated only  $\delta^{18}O_{CO3}$ values for an additional 31 modern specimens. All  $\delta^{18} O_{CO3}$  values were converted from VPDB to VSMOW for comparison with  $\delta^{18}O_{PO4}$  values. For our dataset, the  $\delta^{18}O_{CO3}$  ranged from 23.3% to 30.4%, with an average of 26.9  $\pm$  1.6% (n = 148; SMOW values). The range for  $\delta^{18}O_{PO4}$ values was narrower than that for  $\delta^{18}O_{CO3}$  values, ranging from 20.1% to 24.8%, with an average of 22.8  $\pm$  1.2% (n = 117; SMOW values). The offset between  $\delta^{18}O_{CO3}$  and  $\delta^{18}O_{PO4}$  values ranges from 0.3 to 8.0% with an average of 4.3  $\pm$  1.6%. Pearson's correlation shows a significant but low positive correlation between  $\delta^{18}O$  values from carbonate and phosphate across all specimens (Fig. 2, r = 0.44,  $p = 1.09 \times 10^{-6}$ ). A comparison at the family level demonstrated a stronger positive correlation for Carcharhinidae (n = 49; r = 0.70,  $p = 7.49 \times 10^{-9}$ ). However, other families had weaker correlations than the entire sample set. For example, Carchariidae had extensive variation, which spanned most of the range ( $\delta^{18}O_{CO3}$  ranged 4.6% and  $\delta^{18}O_{PO4}$  ranged 4.0%), but there was very low correlation (r = 0.24, p = 0.09). Other notable families are Lamnidae and Odontaspididae, where all individuals had elevated  $\delta^{18}$ O values in CO<sub>3</sub> and PO<sub>4</sub> components (i.e., plotted together in the upper right quadrant; Fig. 2).

# 3.2. Modern carbon isotope compositions

We generated  $\delta^{13}C$  values of collagen ( $\delta^{13}C_{org}$ ) and carbonate ( $\delta^{13}C_{CO3}$ ) from wild and captive sharks, totaling 151 modern specimens. The wild specimens have  $\delta^{13}C_{org}$  values that range from -20.7% to -11.1%, with an average of  $-14.0\pm1.5\%$  (n =151). There are five individuals with low  $\delta^{13}C_{org}$  values; four of these individuals were part of a captive controlled feeding experiment and were intentionally fed a  $^{13}C$  depleted diet. The mean C:Nweight% of modern samples was  $3.0\pm0.7$  and there was no distinction by family. The  $\delta^{13}C_{CO3}$  values have a wider range, spanning from -5.4% to 10.3%, with an average of  $2.3\pm3.2\%$ 

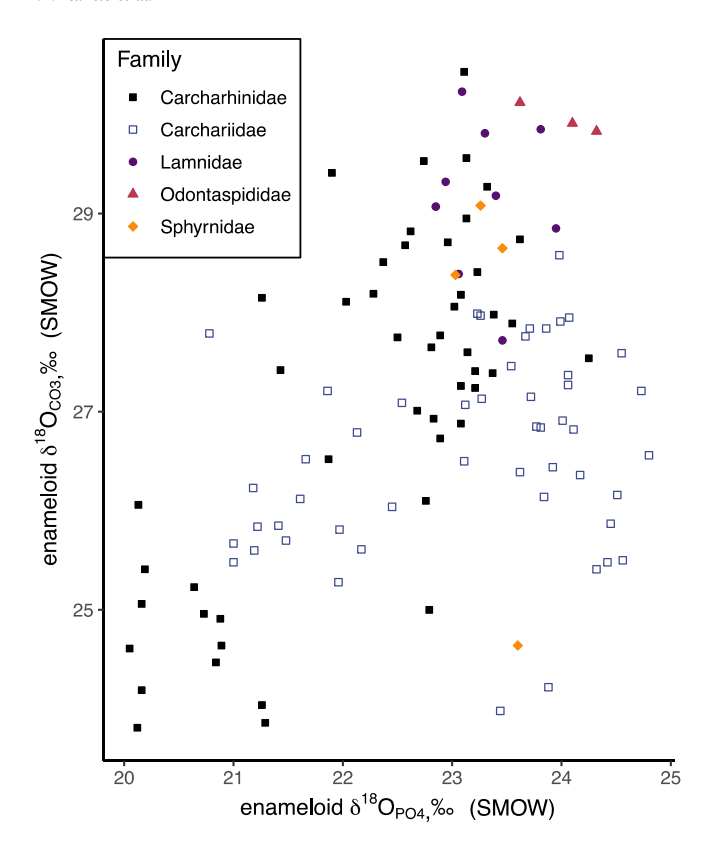


**Fig. 2.** A comparison of enameloid phosphate oxygen ( $\delta^{18}O_{PO4}$ ) and carbonate oxygen ( $\delta^{18}O_{CO3}$ ) isotope composition colored by family. There is weak correlation between these variables (r = 0.44, p = 1.09  $\times$  10<sup>-6</sup>).

(n = 151). Pearson's correlation shows low correlation between  $\delta^{13}C_{org}$ and  $\delta^{13}C_{CO3}$  (Fig. 3, r = 0.17, p = 0.04). Carbon offset ( $\epsilon^*$ ) values have a large range, from 8.9% to 25.3%, with an average of 16.4  $\pm$  3. 4%. Further, this offset has a significant linear correlation with  $\delta^{18}O_{CO3}$ values (Fig. 5,  $R^2 = 0.62$ ,  $p \le 2.2 \times 10^{-16}$ ), but only marginal coherence with  $\delta^{18}O_{PO4}$  values (R<sup>2</sup> = 0.03, p = 0.05). The relationship between  $\varepsilon^*$ and  $\delta^{18}O_{CO3}$  is described by a linear model in Fig. 5,  $\epsilon^* = ((1.54 \pm 0.1) \text{ x})$  $\delta^{18}O_{CO3}$ ) + (22.64  $\pm$  0.5). We did not find distinctions in relationship by family. Comparing the carbonate carbon and oxygen isotope values with Pearson's correlation shows significant correlation (Fig. 4A: r = 0.71, p  $\leq$ 2.2  $\times$  10<sup>-16</sup>). A mixing model to determine proportional inputs of dietary vs. DIC carbon into  $\delta^{13}C_{CO3}$  values (described in §2.6) determined 56% of carbonate carbon was from DIC in seawater. The estimated  $\epsilon_{org}$  values varied across the entire range of -30 to 30 while  $\epsilon_{DIC}$ were more likely positive values. Further, if  $\epsilon_{org} = 0$ , suggesting respired δ<sup>13</sup>C from diet incorporated into enameloid carbonate had a similar isotopic composition to that incorporated into dental collagen, then the proportion of DIC incorporated was less (~40%; Fig. 5). The accompanying  $\epsilon_{org}$  and  $\epsilon_{DIC}$  values are available in the Supplemental Materials (Figs. S3 and S3).

# 3.3. Fossil carbonate analysis

We generated carbonate data ( $\delta^{13}C_{CO3}$  and  $\delta^{18}O_{CO3}$  values) from 54 fossil specimens. The fossils include four geologic periods: Cretaceous (145 Ma – 66 Ma, n=4), Eocene (56 Ma – 33.9 Ma, n=24), Miocene (23.0 Ma – 5.3 Ma, n=18), and Pliocene (5.3 Ma – 2.6 Ma, n=28) (localities are listed in Table 1). For fossil specimens sampled in this study, the  $\delta^{13}C_{CO3}$  values range from –3.4% to 9.6%, with an average of 4.5 ± 3.1% (n=54). The  $\delta^{18}O_{CO3}$  values range from –11.0% to –2.5%, with an average of –4.6 ± 1.7% (n=54; VPDB values). Pearson's correlation shows low correlation between  $\delta^{13}C_{CO3}$  and  $\delta^{18}O_{CO3}$ 

(Fig. 4B: r = 0.10, p = 0.18).

# 3.4. Estimating fossil organic carbon values

Given the strong relationship between  $\epsilon^*$  and  $\delta^{18}O_{CO3}$  values in modern teeth, we apply the linear model from Fig. 5 to fossil teeth and estimate organic  $\delta^{13}C$  values. We refer to these estimated organic carbon isotope compositions as  $\delta^{13}C_{org}^*$  values. The mean and standard deviation of each time bin are as follows: Triassic =  $-14.8 \pm 0.14\%$  (n = 2); Cretaceous =  $-11.5 \pm 3.0\%$  (n = 81); Paleocene =  $-8.3 \pm 1.9\%$  (n = 16); Paleocene/Eocene boundary =  $-24.3 \pm 2.2\%$  (n = 12); Eocene =  $-5.9 \pm 5.8\%$  (n = 39); Miocene =  $-10.0 \pm 4.4\%$  (n = 18); and Pliocene =  $-11.6 \pm 2.3\%$  (n = 33) (Fig. 6). In general, the  $\delta^{13}C_{org}^*$  values from fossil shark teeth had a larger variation and were more  $^{13}C$ -depleted than modern shark teeth (measured  $\delta^{13}C = -14.1 \pm 0.9\%$  [n = 101], this study without captive sharks). One notable exception is the Paleocene/Eocene boundary, which had the lowest mean  $\delta^{13}C_{org}$  estimates recorded for shark teeth.

#### 4. Discussion

We generated a suite of stable isotope values from modern shark teeth to investigate the interrelationships between organic and mineral isotope systems as well as determine paleoecological applications. We discuss patterns between oxygen isotopes in carbonate and phosphate as well as carbon in organic and carbonate substrates. We compare the patterns observed in the extant sharks to those from mammals, a well-studied system. Further, we apply a model based on coupled carbonate – collagen isotope measurements from modern shark teeth to fossil shark teeth to explore the possible implications for paleoecological studies

## 4.1. Oxygen isotopes in shark tooth enameloid

# 4.1.1. Source water

We expected  $\delta^{18}O_{CO3}$  and  $\delta^{18}O_{PO4}$  in enameloid to have a strong linear relationship because both components are thought to form in equilibrium with the same source (i.e., body water) during enameloid mineralization. However, we found only a weak correlation between  $\delta^{18}O_{CO3}$  and  $\delta^{18}O_{PO4}$  values in shark tooth enameloid (Fig. 2), which suggests these components are recording, to a degree, different signals. Experiments with synthetic apatite minerals show that  $\delta^{18}O_{CO3}$  values are controlled by a kinetic fractionation process that involves the  $\delta^{18}$ O of water and temperature at which the reaction occurs (Lecuyer et al., 2010). Therefore, in living organisms it is expected that biomineralized materials are formed in equilibrium with body water. Previous studies with mammals confirmed that enamel  $\delta^{18}\text{O}$  values reflect  $\delta^{18}\text{O}$  values of ingested water (Iacumin et al., 1996; Longinelli, 1984; Luz and Kolodny, 1985; Podlesak et al., 2008). Since mammals have a constant body temperature, the  $\delta^{18}O_{CO3}$  and  $\delta^{18}O_{PO4}$  values of bioapatite have a linear relationship with only slight variations in the reported equations and error (Bryant et al., 1996; Chenery et al., 2012; Göhring et al., 2019; Iacumin et al., 1996; Martin et al., 2008; Pellegrini et al., 2011; Zazzo et al., 2004b). Tooth growth patterns and oxygen isotope values in mammals have also been modeled to reconstruct seasonal environmental conditions (Green et al., 2018a, 2018b, 2022; Passey et al., 2005; Trayler and Kohn, 2017).

In ectotherms, the oxygen isotope composition of bioapatite reflects both body water  $\delta^{18}{\rm O}$  values and the temperature at time of mineralization. Empirical relationships for environmental water  $\delta^{18}{\rm O}$  values, temperature, and  $\delta^{18}{\rm O}_{PO4}$  values in biological apatite are established for fish (Kolodny et al., 1983; Longinelli and Nuti, 1973). This relationship was applied to sharks by Vennemann et al. (2001), which resulted in expected temperature estimates of multiple species and their habitats. The equation was later revised with a study of captive fish (Pucéat et al., 2010) and revised again most recently by Lécuyer et al. (2013). Our

results from shark enameloid also support the relationship between  $\delta^{18}O_{PO4}$  values and environmental conditions.

If both phosphate and carbonate oxygen isotope compositions are forming in equilibrium with body water, similar to mammals,  $\delta^{18} O_{CO3}$  and  $\delta^{18} O_{PO4}$  values would have a strong linear relationship. However, our values of  $\delta^{18} O_{CO3}$  and  $\delta^{18} O_{PO4}$  have low correlation (Fig. 2, r=0.44,  $p=1.09\times 10^{-6}$ ). This result is consistent with the larger variation in  $\delta^{18} O_{CO3}$  compared to  $\delta^{18} O_{PO4}$  values first reported in Vennemann et al. (2001). One explanation is the incorporation of oxygen from DIC into the carbonate ion, as DIC has multiple ions with associated oxygen atoms (CO<sub>2</sub>, CO $_3^{2-}$ , HCO $_3^{-}$ ). Further, there is evidence from invertebrates that oxygen isotope fractionation decreases with pH (Zeebe, 2007). With multiple studies showing a strong relationship between source water, temperature, and  $\delta^{18} O_{PO4}$  in fish, it is most likely that the variation we see in sharks is caused by an additional factor affecting  $\delta^{18} O_{CO3}$  values.

## 4.1.2. Taxonomic patterns

Despite having low correlation across the sampled population, we found patterns in  $\delta^{18}O_{CO3}$  and  $\delta^{18}O_{PO4}$  values when examined by taxonomic family. Carcharhinid sharks (*Carcharhinus brevipinna* n=1, *C. leucas* n=19, *C. limbatus* n=5, *C. obscurus* n=5, *C. plumbeus* n=15, *Galeocerdo cuvier* n=9) have a strong and significant correlation between  $\delta^{18}O_{CO3}$  and  $\delta^{18}O_{PO4}$  (r=0.70,  $p=7.49\times 10^{-9}$ ). In contrast, these values in lamnid sharks (*Lamna ditropis* n=3, *Carcharodon carcharias* n=6) do not correlate (r=-0.06, p=0.88) and instead group together with elevated  $\delta^{18}O_{CO3}$  values (Fig. 2). This pattern is likely due to their partial endothermy, a form of thermoregulation that allows retention of some metabolic heat to elevate body temperature above their environment (Goldman, 1997; Griffiths et al., 2023).

The odontaspidid sharks (*Carcharias taurus n* = 54, *Odontaspis ferox* n = 3) also show an interesting pattern, with differentiation by species and habitat. In *C. taurus*, wild-caught and aquarium-kept individuals differentiate in  $\delta^{18}O_{PO4}$  values, as expected given stable water temperatures in captivity, but not in  $\delta^{18}O_{CO3}$  values (Fig. 2). This pattern could be due to water treatment or additives at the aquarium that affect DIC isotope composition or due to the migratory pattern of wild *C. taurus*. Individuals sampled are part of a population in Delaware Bay that spends time in the low salinity waters of the bay and migrates along the coastal shelf (Kneebone et al., 2012, 2014; McCormack et al., 2023; Teter et al., 2015). The *O. ferox* individuals have a similar range in  $\delta^{18}O_{PO4}$  values as the wild *C. taurus*, but differentiate in  $\delta^{18}O_{CO3}$  values, possibly due to their habitat preference for deeper water (Compagno, 2001).

## 4.1.3. Oxygen offset as a metric for diagenesis

The carbonate-phosphate oxygen isotope spacing ( $\delta^{18}O_{CO3}$  - $\delta^{18}O_{PO4}$ ) has been proposed as diagnostic tool for diagenesis in fossils (e. g., Kohn and Cerling, 2002). Previous studies on mammalian teeth suggest an expected offset of ~9% in unaltered samples and deviation from this range is interpreted as alteration (Bryant et al., 1996; Eagle et al., 2011; Iacumin et al., 1996; Martin et al., 2008). Modern mammal studies generally report standard deviations of <1% for this offset. Despite close correlation between the two variables in mammals, a few studies still caution against reliance on this metric. For example, one study found an average spacing of 8.4  $\pm$  0.7‰, but a large intra-tooth variation of ~2% (Martin et al., 2008). A literature review of mammalian oxygen isotope spacing concluded that despite strong correlation, the amount of variability in spacing means this measurement should not be used a diagnostic tool for diagenesis until the water source of bioapatite mineralization is better understood (Pellegrini et al., 2011).

More recent studies suggest that this variability in oxygen isotope spacing may be related to species or diet-specific differences (Göhring et al., 2019) or impacted by seasonality (Fraser et al., 2021). Enameloid in bony fish has a reported offset of 8.1–11.0% in modern specimens and 6.8–11.7% in Holocene specimens (Sisma-Ventura et al., 2019).

Similarly, this offset has a much larger range in modern sharks (Vennemann et al., 2001 range: 6.0–11.8% with an average of 9.1  $\pm$  1.5%; our data range: 0.3–7.5%). Given the lack of strong correlation between  $\delta^{18}$ O values from carbonate and phosphate in our dataset as well as the larger variation in offset for modern sharks, we do not recommend this metric as a diagnostic measure of diagenesis in shark teeth.

# 4.2. Complexity of $\delta^{13}C_{CO3}$ values from shark teeth

The carbon isotope composition in aquatic and marine biominerals potentially reflects dissolved inorganic carbon (DIC) exchanged or adsorbed during mineralization. Our results demonstrate low correspondence between  $\delta^{13} C_{CO3}$  and  $\delta^{13} C_{org}$  values (Fig. 3) in modern shark teeth, which suggests that  $\delta^{13}C_{CO3}$  does not represent diet. However, there are other marine organisms where  $\delta^{13}C_{CO3}$  values record diet and environmental conditions. For example,  $\delta^{13}C_{CO3}$  values of corals form in equilibrium with environmental water and vary with DIC and photosynthesis (McConnaughey et al., 1997); and the  $\delta^{13}C_{CO3}$  values of fish otoliths are a combined signal of diet, DIC, and metabolism that is best represented with a two-component mixing model (Chung et al., 2019). We adapted the Chung et al. (2019) mixing model with two fractionation factors and estimated the contribution of environmental carbon (DIC) to the  $\delta^{13}C_{\text{CO3}}$  values in our extant shark teeth. Our model assumed that the dental collagen  $\delta^{13}C$  values were analogous to the respired carbon incorporated into enameloid carbonate, which is supported by the offset in  $\delta^{13}C$  and  $\delta^{15}N$  values from diet and incorporation rates determined for carbon and nitrogen (Zeichner et al., 2017). Regardless, if there are two fractionation factors (i.e.,  $\epsilon_{org}$  and  $\epsilon_{DIC}$ ) or no additional fractionation between organic carbon incorporated into dental collagen and enameloid carbonate, seawater DIC contribution estimates are substantial and likely 40%-70% based on our isotopic results and model assumptions (more results and discussion available in Supplemental Materials).

Further, this study includes individuals from a captive feeding study

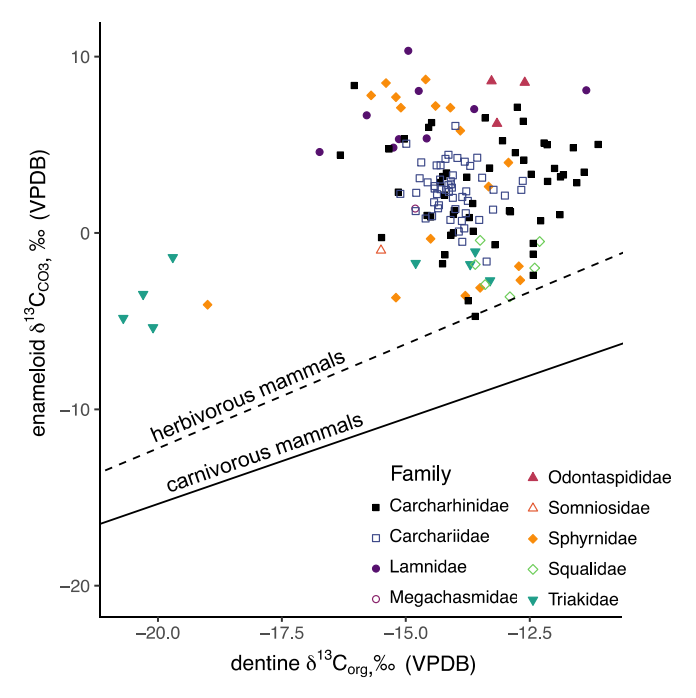


**Fig. 3.** Dentine organic carbon  $(\delta^{13}C_{org})$  compared to enameloid carbonate carbon  $(\delta^{13}C_{CO3})$  isotope values colored by family. There is no correlation between these variables in contrast to results from mammals, which is shown by the lines. The dashed line is the best fit for herbivorous mammals and solid line is the best fit for carnivorous mammals  $(r^2 > 0.89)$  and p-values < 0.0001; Codron et al., 2018).

(Kim et al., 2012b), which supports the explanation that  $\delta^{13}C_{CO3}$  values do not solely represent diet in sharks. The leopard sharks (Triakidae) were kept in similar water conditions but fed two isotopically distinct diets (i.e., squid  $\delta^{13}C=-18.5\pm0.5\%$  and tilapia  $\delta^{13}C=-23.2\pm$ 0.9%; Kim et al., 2012b). Although the sharks fed tilapia had distinct  $\delta^{13}C_{org}$  values (~6% lower), their  $\delta^{13}C_{CO3}$  values were more similar to the squid-fed leopard sharks (~2% lower) and within the range of wild sharks. Having isotopically distinct diets and  $\delta^{13}C_{org}$  values, yet similar  $\delta^{13}C_{CO3}$  values indicates the carbonate substrate is not tracking diet with high fidelity. However, all the captive leopard sharks shared the same water conditions, which suggests the incorporation of an environmental factor, such as DIC, similar to fish otoliths. Similar results were found by Leuzinger et al. (2023) who hypothesize that these elevated  $\delta^{13}C_{CO3}$ values may be a product of fractionation during biomineralization processes. To further investigate enameloid  $\delta^{13}$ C values in carbonate, future studies could compare dentine  $\delta^{13}C_{org}$  and  $\delta^{13}C_{CO3}$  as well as enameloid  $\delta^{13}C_{CO3}$  and  $\delta^{13}C_{org}$  values, however the size of teeth in this study and analytical instrumentation limits of our facility precluded that

We also observed that this phenomenon was limited to oxygen isotope composition of carbonate and did not affect phosphate. There was a strong positive relationship of  $\varepsilon^*$  with  $\delta^{18}O_{CO3}$  values (Fig. 5:  $r^2$  =  $0.62, p < 2.2 \times 10^{-16}$ ), but not with  $\delta^{18}O_{PO4}$  values ( $r^2 = 0.04, p = 0.03$ ), which suggests that the unusual carbon isotope values in shark enameloid could be associated with carbonate ion (CO<sub>3</sub><sup>-2</sup>) substitutions rather than isolated to  $^{13}\mathrm{C}$  fractionation in biomineralization. If during the enameloid maturation process DIC (in the form of  $CO_3^{2-}$ ) is incorporated or exchanged in the mineral matrix, then it would affect both  $\delta^{13}C_{CO3}$ and  $\delta^{18}O_{CO3}$  values. This process is likely temperature dependent; the water temperature would affect the surrounding water pCO2, differential between blood and seawater pCO2, and fractionation factors as seawater DIC is incorporated into the mineral matrix. Despite the enigmatic nature of isotope compositions in shark enameloid, we used the linear relationship between  $\epsilon^*$  with  $\delta^{18}O_{CO3}$  values to develop a predictive model and estimate the  $\delta^{13} C_{\text{org}}$  values of fossil shark teeth. With carbonate isotope composition, the linear regression can estimate δ<sup>13</sup>C<sub>org</sub> values, which has application for paleoecological studies of carbon cycling, diet, and food web dynamics of ancient marine ecosystems.

# 4.3. Estimated fossil organic carbon values

The carbon isotope composition of marine ecosystems varied through geologic time depending on carbon cycling processes, but inferences rely mostly on residual organic matter in sediments (Jenkyns, 2010) and the inorganic carbonate record (Prokoph et al., 2008). Organic carbon in protein substrates, such as dental and bone collagen, decays quickly and typically cannot be analyzed beyond 100,000 years (Clementz, 2012), however recent studies successfully analyzed nitrogen isotope composition from mineral-bound organics in enamel(oid) (Kast et al., 2022; Leichliter et al., 2021). We estimated  $\delta^{13}C_{org}$  values for fossil shark teeth using a linear model based on modern shark teeth (Fig. 5).

The average  $\delta^{13}C_{org}^*$  value decreases over time from the Eocene towards modern (Fig. 6) so that Pliocene sharks are most similar to modern sharks. A declining trend is also documented in inorganic carbon isotope record measured in benthic foraminifera (Zachos et al., 2001), although the magnitude of change (~1‰) is smaller than that of our  $\delta^{13}C_{org}^*$  values. Records of organic carbon isotopes in sedimentary rocks show a larger magnitude of variation through time than the carbonate record (Khozyem et al., 2021; Wang et al., 1997), although still not nearly as large as the change that we see in the samples from the Paleocene/Eocene boundary. Similar to what is seen in our data, the Cretaceous has been found to have a higher carbon isotopic baseline (Cullen et al., 2023). The Eocene and Paleocene-Eocene boundary (P/E) are both anomalies to the trend. The P/E has the lowest mean  $\delta^{13}C_{org}^*$ 

value ( $-24.3 \pm 2.2\%$ ) while the Eocene has the most variability and highest mean  $\delta^{13}C_{org}^*$  value ( $-3.3 \pm 5.9\%$ ). Over longer time spans, both the organic and inorganic carbon isotope records have been remarkably stable, with deviations over the last  $\sim 3.5$  billion years averaging  $\sim 25\%$  (Garcia et al., 2021).

The carbonate isotope compositions of fossil shark teeth may have some alteration and this approach of  $\delta^{13}C_{org}^*$  values must be further refined before applications to paleoceanography or paleoecology. While the bioapatite of enameloid may preserve the phosphate isotope composition, there are previous studies that suggest carbonate is more vulnerable to diagenesis (Zazzo et al., 2004a). The degradation of organics within dentine can result in ion exchange and recrystallization of apatite (Keenan, 2016). Additionally, Feichtinger et al. (2020) revealed that fossilized teeth preserved microbes that bored into the organic and mineralized tissue through collagen fibers, potentially altering the organic collagen and inorganic carbonate carbon isotopic compositions. Even when using the mineral portion of dentine, the bonds between C-O are weaker compared to phosphate, as carbonate is readily dissolved from apatite and is also prone to analytical bias (Demény et al., 2019; Lee-Thorp, 2002). The contrasting patterns between  $\delta^{13}$ C and  $\delta^{18}$ O values from carbonate in modern vs. fossils specimens (Fig. 4A vs. B) suggest caution in interpretations from carbonate isotope

The intriguing Eocene  $\delta^{13}C_{org}^*$  values may reflect distinct environmental conditions during this time. For example, the Eocene  $\delta^{13}C_{org}^*$ values are widely variable and <sup>13</sup>C-enriched compared to other epochs. One possible cause is variation in salinity; many of our samples are from the Eureka Sound Formation on Banks Island in the Arctic where  $\delta^{18}O_{CO3}$  values from shark enameloid indicate brackish water (Kim et al., 2014). Salinity affects both concentration and  $\delta^{13}$ C of DIC (Bakker et al., 1999; Gillikin et al., 2006). Differences in  $\delta^{13}C_{DIC}$  values caused by low salinity would affect  $\delta^{13} C_{\text{org}}$  values of autotrophs at the base of the food web and cascade to predators like sharks. Secondly, the Eocene is known for greenhouse climate conditions with high mean global temperatures, high concentrations of atmospheric CO2, and punctuated climate events characterized by negative carbon isotope excursions (Zachos et al., 2008). These climate events include longer events such as the Early Eocene Climatic Optimum (EECO) and more rapid events known as hyperthermals such as the Paleocene-Eocene Thermal Maximum (PETM), the best studied and most extreme Eocene hyperthermal. These relatively short but intense perturbations to inorganic carbon could cause the larger variation in  $\delta^{13}C_{org}^*$  values estimated from the linear regression from modern teeth.

The possibility to estimate  $\delta^{13} C_{org}$  values based on carbonate SIA in shark teeth presents opportunities to extend paleo SIA applications beyond environmental reconstruction to exploring ecological topics like food web dynamics. Inorganic carbon isotope values are rarely used or reported in the literature due to their abnormal values. Besides this study, there is only one published dataset of inorganic carbon isotope values for modern sharks (Vennemann et al., 2001). There are a few paleontological studies reporting  $\delta^{13}C_{CO3}$  values for fossil shark teeth; however, these values were not used to make paleoecological interpretations (Aguilera et al., 2017; Kocsis et al., 2014; Kolodny and Luz, 1992; Ounis et al., 2008; Van Baal et al., 2013). Here, we propose a model to estimate dietary carbon based on carbonate isotope composition of shark enameloid. These estimates would allow us to investigate questions about nearshore vs. offshore environments, nutrient-rich upwelling regions, and productivity regimes with comparisons between modern sharks and the fossil record. However, we want to reiterate our caution in using this model in its current form and encourage further investigation, especially given the discrepancy in the association between  $\delta^{13}C_{CO3}$  and  $\delta^{18}O_{CO3}$  in modern and ancient shark teeth (Fig. 4 A

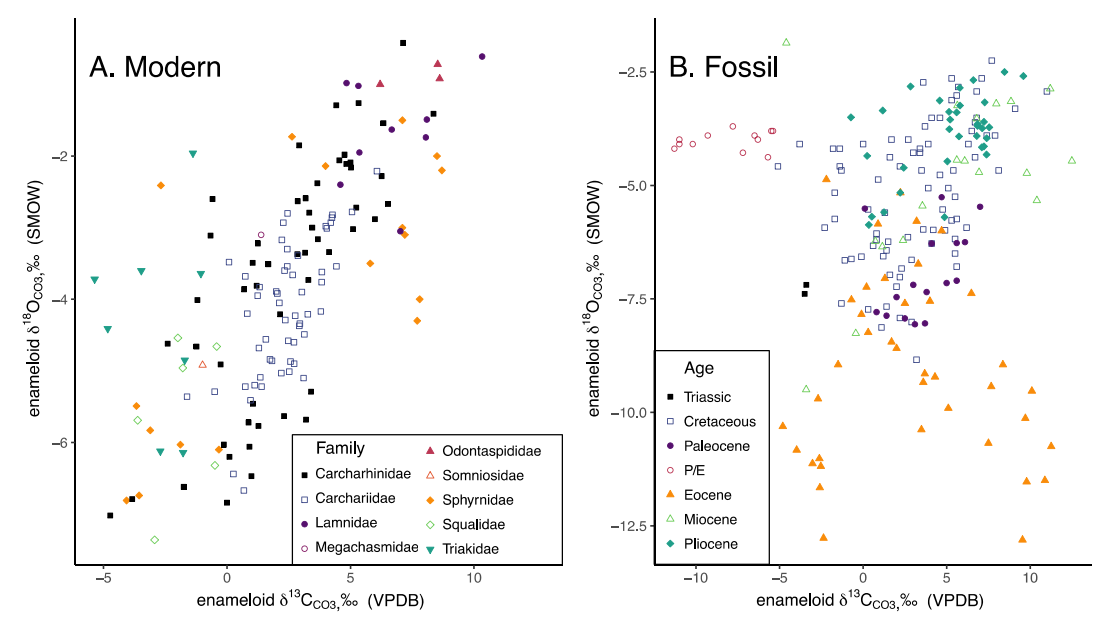


Fig. 4. Carbonate carbon ( $\delta^{13}C_{CO3}$ ) vs. carbonate oxygen ( $\delta^{18}O_{CO3}$ ) isotope values for A) modern teeth (r = 0.71,  $p \le 2.2 \times 10^{-16}$ ) and B) fossil teeth (r = 0.10, p = 0.18). Data points in A colored by family and in B colored by geologic age, "P/E" are samples from the Paleocene/Eocene boundary.

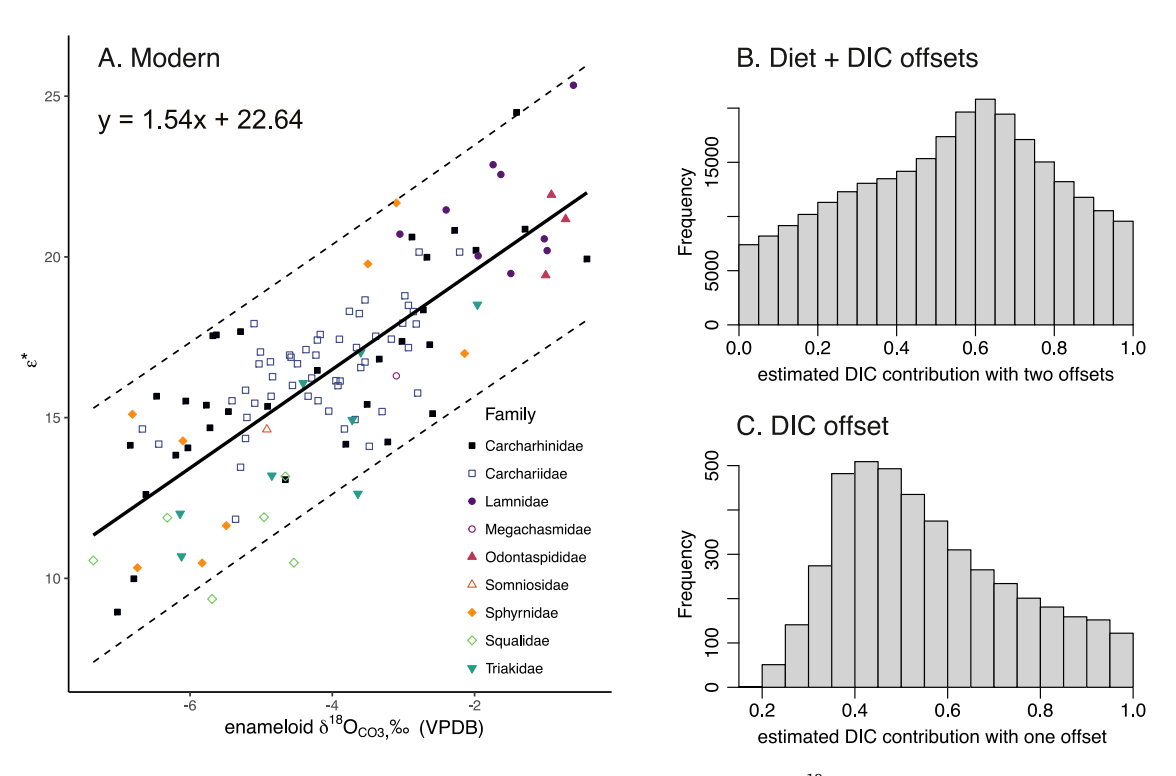


Fig. 5. A) The carbon fractionation ( $\epsilon = 1000*ln(\alpha)$ ) compared to carbonate oxygen isotope composition ( $\delta^{18}O_{CO3}$ ). A linear regression of the data is in black ( $y = 1.54 \times + 22.64$ ,  $R^2 = 0.62$ ,  $p \le 2.2 \times 10^{-16}$ ), with the 95% confidence interval shaded. The dashed lines represent the 95% prediction interval. Points are colored by family. B & C) Estimates of DIC contribution from adapted Chung et al. (2019) mixing model. Results for modern data in this study when B) two offsets are used for respired dietary carbon and seawater DIC incorporation or C) there is only one offset for seawater DIC (assuming respired dietary carbon has no additional offset from dental collagen) during enameloid mineralization.

# 5. Conclusions

In conclusion, we compiled and analyzed the largest dataset to date of stable isotope values comparing multiple substrates in modern and fossil shark teeth. This study provides a foundation for the use of shark teeth beyond environmental reconstructions to examine shark paleoecology. Due to poor correlation between  $\delta^{18}O_{CO3}$  and  $\delta^{18}O_{PO4}$  values,

we suggest only using  $\delta^{18}O_{PO4}$  values from shark enameloid as a proxy for temperature or water  $\delta^{18}O$  values. Additionally, the carbonate-phosphate oxygen isotope spacing  $(\delta^{18}O_{CO3}$  -  $\delta^{18}O_{PO4})$  should not be used as a diagnostic tool for diagenetic alteration in shark teeth because there is a significant amount of variation among modern teeth, which have no possibility for diagenetic alteration. In sharks,  $\delta^{13}C_{CO3}$  values do not correlate with  $\delta^{13}C_{org}$  values and therefore does not reflect diet.

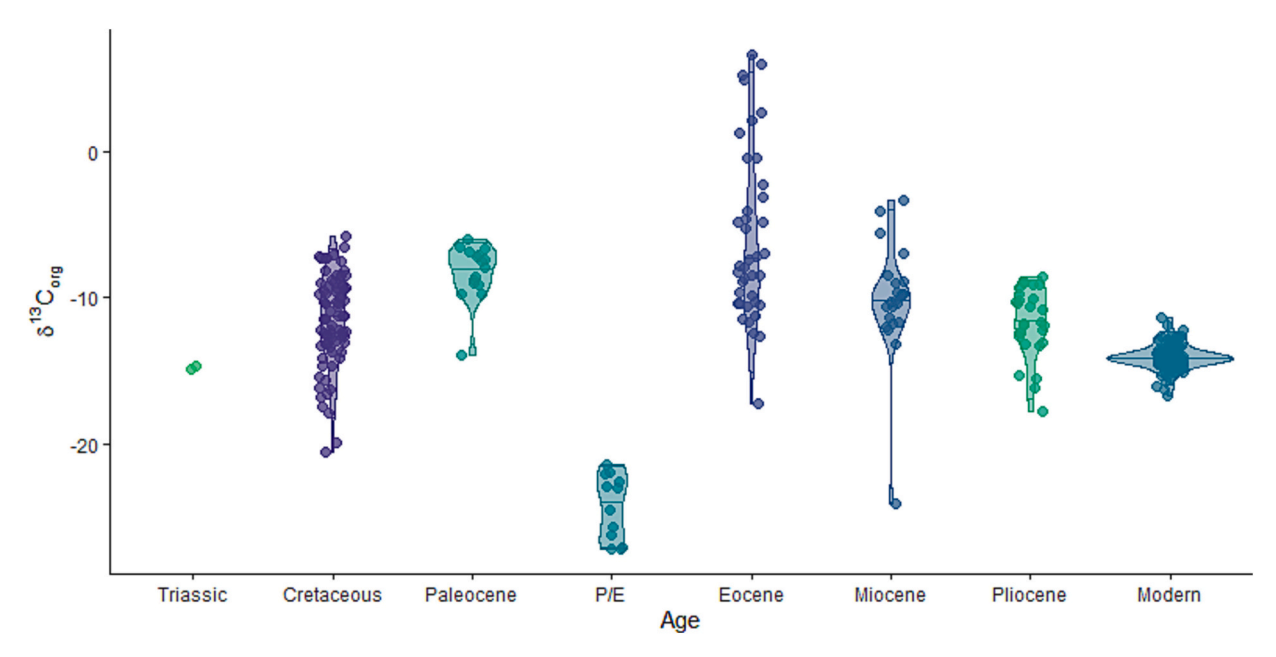


Fig. 6. Organic carbon isotope values by geologic age of teeth. Modern values are measured from analysis of dental collagen and fossil values are estimated using the regression equation from Fig. 5 ( $\delta^{13}C_{org}^*$ ). Includes generated for this study and data compiled from literature (Aguilera et al., 2017; Kocsis et al., 2014; Kolodny and Luz, 1992; Ounis et al., 2008; Van Baal et al., 2013).

Instead,  $\delta^{13}C_{CO3}$  values likely reflect a combined diet and DIC signal, similar to fish otoliths. This hypothesis is supported by the relationship between carbon fractionation ( $\epsilon^*$ ) and  $\delta^{18}O_{CO3}$  values. The model from this relationship was tested on a fossil dataset that included specimens from the Triassic, Cretaceous, Paleocene, Eocene, Miocene, and Pliocene. It allows estimation of  $\delta^{13}C_{org}{}^*$  values from fossil tooth enameloid, which indicate  $^{13}C$  enrichment through time. Although preliminary and likely affected by diagenesis, this trend provides a basis to investigate carbon cycling and food web dynamics in ancient marine environments using fossil shark teeth.

# CRediT authorship contribution statement

Molly E. Karnes: Conceptualization, Data curation, Formal analysis, Investigation, Methodology, Project administration, Validation, Visualization, Writing – original draft, Writing – review & editing. Rachel L. Chan: Conceptualization, Data curation, Investigation, Validation, Writing – review & editing. Jonathon P. Kuntz: Investigation, Writing – review & editing. Michael L. Griffiths: Funding acquisition, Resources, Writing – review & editing. Kenshu Shimada: Data curation, Funding acquisition, Resources, Writing – review & editing. Martin A. Becker: Funding acquisition, Resources, Writing – review & editing. Robert A. Eagle: Funding acquisition, Writing – review & editing. Shawn Miller: Data curation, Writing – review & editing. Shawn Miller: Data curation, Writing – review & editing. Sora L. Kim: Conceptualization, Funding acquisition, Investigation, Methodology, Resources, Supervision, Visualization, Writing – review & editing.

# **Declaration of Competing Interest**

The authors declare the following financial interests/personal relationships which may be considered as potential competing interests:

Michael L Griffiths reports financial support was provided by National Science Foundation. Robert A Eagle reports financial support was provided by National Science Foundation. Kenshu Shimada reports financial support was provided by National Science Foundation. Sora L Kim reports financial support was provided by National Science Foundation. Martin A Becker reports financial support was provided by

National Science Foundation.

#### Data availability

All data used in this study is available in the supplemental data table and DRYAD data repository (doi:https://doi.org/10.6071/M3067S).

## Acknowledgments

Funding: This research was supported by a National Science Foundation (NSF) Sedimentary Geology and Paleobiology Award to M.L.G. and M.A.B. (#1830581), R.A.E. (#1830638), K.S. (#1830858), S.L.K. (#1830480), and UROP from the Office of Undergraduate Research at the University of Utah. M.E.K. was partially supported by NSF Office of Polar Programs Award to S.L.K (#1842049). A NSF CAREER award to S. L.K. (#2239981) supported the final stages of this research.

We thank the following individuals for curating and loaning us the reposited specimens for destructive sampling: Stephen Godfrey and John Nance (Calvert Marine Museum, Solomons, Maryland, USA), Thomas Deméré and Kesler Randall (San Diego Natural History Museum, San Diego, California, USA), Arnold Suzumoto (Bernice P. Bishop Museum, Honolulu, Hawaii, USA), Caleb McMahan (Field Museum of Natural History, Chicago, Illinois, USA), and Katrina M. Derieg (Natural History Museum of Utah, Salt Lake City, Utah, USA).

We would like to thank the illustrator of the sketch in Fig. 1A, Sarah Baird, and Simon De Marchi who provided the hammerhead jaw for Sarah to reference in her drawing. Further, we appreciated the advice and feedback from Thure Cerling during this project and assistance with mixing model dynamics from Justin Yeakel.

# Appendix A. Supplementary data

Supplementary data to this article can be found online at https://doi.org/10.1016/j.palaeo.2023.111943.

#### References

Aguilera, O., Luz, Z., Carrillo-Briceño, J.D., Kocsis, L., Vennemann, T.W., De Toledo, P. M., Nogueira, A., Amorim, K.B., Moraes-Santos, H., Polck, M.R., Ruivo, M.L.,

- Linhares, A.P., Monteiro-Neto, C., 2017. Neogene sharks and rays from the Brazilian 'Blue Amazon'. PLoS One 12, 1–34. https://doi.org/10.1371/journal.pone.0182740.
- Amiot, R., Göhlich, U.B., Lécuyer, C., de Muizon, C., Cappetta, H., Fourel, F., Héran, M. A., Martineau, F., 2008. Oxygen isotope compositions of phosphate from Middle Miocene-early Pliocene marine vertebrates of Peru. Palaeogeogr. Palaeoclimatol. Palaeoecol. 264, 85–92. https://doi.org/10.1016/j.palaeo.2008.04.001.
- Bakker, D.C.E., De Baar, H.J.W., De Jong, E., 1999. The dependence on temperature and salinity of dissolved inorganic carbon in East Atlantic surface waters. Mar. Chem. 65, 263–280. https://doi.org/10.1016/S0304-4203(99)00017-1.
- Berkovitz, B.K.B., Shellis, R.P., 2017. The Teeth of Non-Mammalian Vertebrates. https://doi.org/10.1016/C2014-0-02210-1.
- Blumenthal, S.A., Cerling, T.E., Chritz, K.L., Bromage, T.G., Kozdon, R., Valley, J.W., 2014. Stable isotope time-series in mammalian teeth: in situ δ 18 O from the innermost enamel layer. Geochim. Cosmochim. Acta. https://doi.org/10.1016/j.gca.2013.09.032.
- Bryant, J.D., Koch, P.L., Froelich, P.N., Showers, W.J., Genna, B.J., 1996. Oxygen isotope partitioning between phosphate and carbonate in mammalian apatite. Geochim. Cosmochim. Acta 60, 5145–5148.
- Casey, M.M., Post, D.M., 2011. The problem of isotopic baseline: Reconstructing the diet and trophic position of fossil animals. Earth-Sci. Rev. 106, 131–148. https://doi.org/ 10.1016/j.earscirev.2011.02.001.
- Cerling, T.E., Harris, J.M., 1999. Carbon isotope fractionation for ecological mammals and implications for ecological and and paleoecological studies. Oecologia 120, 347–363.
- Chan, R.L., 2022. Modeling δ<sup>18</sup>O of Phosphate and Carbonate from Recent Shark Teeth and Marine Conditions from Fossilized Shark Teeth. University of California Merced. Master's Thesis.
- Chenery, C.A., Pashley, V., Lamb, A.L., Sloane, H.J., Evans, J.A., 2012. The oxygen isotope relationship between the phosphate and structural carbonate fractions of human bioapatite. Rapid Commun. Mass Spectrom. 309–319 https://doi.org/ 10.1002/rcm.5331.
- Chung, M.T., Trueman, C.N., Godiksen, J.A., Grønkjær, P., 2019. Otolith δ13C values as a metabolic proxy: Approaches and mechanical underpinnings. Mar. Freshw. Res. 70, 1747–1756. https://doi.org/10.1071/MF18317.
- Clementz, M.T., 2012. New insight from old bones: Stable isotope analysis of fossil mammals. J. Mammal. 93, 368–380. https://doi.org/10.1644/11-MAMM-S-179.1.
- Codron, D., Clauss, M., Codron, J., Tütken, T., 2018. Within trophic level shifts in collagen–carbonate stable carbon isotope spacing are propagated by diet and digestive physiology in large mammal herbivores. Ecol. Evol. 8, 3983–3995. https:// doi.org/10.1002/ece3.3786.
- Compagno, L.J.V., 2001. Order LAMNIFORMES Mackerel sharks. In: Sharks of the World: An Annotated and Illustrated Catalogue of Shark Species Known to Date, pp. 51–67.
- Cullen, T.M., Longstaffe, F.J., Wortmann, U.G., Huang, L., Evans, D.C., 2023. Anomalous 13C enrichment in Mesozoic vertebrate enamel reflects environmental conditions in a "vanished world" and not a unique dietary physiology. Paleobiology 1–15. https:// doi.org/10.1017/pab.2022.43.
- Demény, A., Gugora, A.D., Kesjár, D., Lécuyer, C., Fourel, F., 2019. Stable isotope analyses of the carbonate component of bones and teeth: the need for method standardization. J. Archaeol. Sci. 109 https://doi.org/10.1016/j.jas.2019.104979
- DeNiro, M.J., Epstein, S., 1978. Influence of diet on the distribution of carbon isotopes in animals\*. Geochim. Cosmochim. Acta 42, 495–506. https://doi.org/10.1002/
- Eagle, R.A., Tütken, T., Martin, T.S., Tripati, A.K., Fricke, H.C., Connely, M., Cifelli, R.L., Eiler, J.M., 2011. Dinosaur body temperatures determined from isotopic (13C-18O) ordering in fossil biominerals. Science 333, 443–445. https://doi.org/10.1126/ ccipres.1206102
- Enax, J., Prymak, O., Raabe, D., Epple, M., 2012. Structure, composition, and mechanical properties of shark teeth. J. Struct. Biol. 178, 290–299. https://doi.org/10.1016/j. ich.2012.03.012
- Feichtinger, I., Lukeneder, A., Topa, D., Kriwet, J., Libowitzky, E., Westall, F., 2020. Fossil microbial shark tooth decay documents in situ metabolism of enameloid proteins as nutrition source in deep water environments. Sci. Rep. 10, 1–11. https://doi.org/10.1038/s41598-020-77964-5.
- Fellah, C., Douillard, T., Maire, E., Meille, S., Reynard, B., Cuny, G., 2021. 3D microstructural study of selachimorph enameloid evolution. J. Struct. Biol. 213 https://doi.org/10.1016/j.jsb.2020.107664.
- Francillon-Vieillot, H., de Buffrénil, V., Castanet, J., Géraudie, J., Meunier, F.J., Sire, J.Y., Zylberberg, L., de Ricqlès, A., 1990. Microstructure and mineralization of vertebrate skeletal tissues. In: Skeletal Biomineralization: Pattern, Processes and Evolutionary Trends, vol. I, pp. 471–530.
- Fraser, D., Kim, S.L., Welker, J.M., Clementz, M.T., 2021. Pronghorn (Antilocapra americana) enamel phosphate δ18O values reflect climate seasonality: Implications for paleoclimate reconstruction. Ecol. Evol. 11, 17005–17021. https://doi.org/10.1002/ece3.8337.
- Garcia, A.K., Cavanaugh, C.M., Kacar, B., 2021. The curious consistency of carbon biosignatures over billions of years of Earth-life coevolution. ISME J. 15, 2183–2194. https://doi.org/10.1038/s41396-021-00971-5.
- Gillikin, D.P., Lorrain, A., Bouillon, S., Willenz, P., Dehairs, F., 2006. Stable carbon isotopic composition of Mytilus edulis shells: relation to metabolism, salinity, 813CDIC and phytoplankton. Org. Geochem. 37, 1371–1382. https://doi.org/ 10.1016/j.orggeochem.2006.03.008.
- Gillis, J.A., Donoghue, C.J., 2007. The homology and phylogeny of chondrichthyan tooth enameloid. J. Morphol. 268, 33–49. https://doi.org/10.1002/jmor.
- Glas, J.E., 1962. Studies on the ultrastructure of dental enamel. VI. Crystal chemistry of shark's teeth. Odont. Revy 13, 315–326.

- Goettig, P., Magdolen, V., Brandstetter, H., 2010. Natural and synthetic inhibitors of kallikrein-related peptidases (KLKs). Biochimie 92, 1546–1567. https://doi.org/ 10.1016/j.biochi.2010.06.022.
- Göhring, A., Carnap-Bornheim, C., Hilberg, V., Mayr, C., Grupe, G., 2019. Diet and species-specific oxygen isotope relationship and isotope spacing between structural carbonate and phosphate in archaeological mammalian bones. Archaeol. Anthropol. Sci. 11, 2467–2487.
- Goldman, K.J., 1997. Regulation of body temperature in the white shark, Carcharodon carcharias. J. Comp. Physiol. B. 167, 423–429.
- Green, D.R., Green, G.M., Colman, A.S., Bidlack, F.B., Tafforeau, P., Smith, T.M., 2017. Synchrotron imaging and Markov Chain Monte Carlo reveal tooth mineralization patterns. PLoS One 1–16.
- Green, D.R., Olack, G., Colman, A.S., 2018a. Determinants of blood water δ 18 O variation in a population of experimental sheep: Implications for paleoclimate reconstruction. Chem. Geol. 485, 32–43. https://doi.org/10.1016/j.chemgeo.2018.03.034.
- Green, D.R., Smith, T.M., Green, G.M., Bidlack, F.B., Tafforeau, P., Colman, A.S., 2018b. Quantitative reconstruction of seasonality from stable isotopes in teeth. Geochim. Cosmochim. Acta 235, 483–504. https://doi.org/10.1016/j.gca.2018.06.013.
- Green, D.R., Avila, J.N., Smith, T.M., Cote, S., Dirks, W., Lee, D., Poulsen, C.J., Williams, I.S., 2022. Fine-scaled climate variation in equatorial Africa revealed by modern and fossil primate teeth. PNAS 119. https://doi.org/10.1073/ pnas.2123366119/-/DCSupplemental.Published.
- Griffiths, M.L., Eagle, R.A., Kim, S.L., Flores, R.J., Becker, M.A., Maisch, H.M.I., Trayler, R.B., Chan, R.L., McCormack, J., Akhtar, A.A., Tripati, A.K., Shimada, K., 2023. Endothermic physiology of extinct megatooth sharks. Proc. Natl. Acad. Sci. 120, 8. https://doi.org/10.1073/pnas.
- Hättig, K., Stevens, K., Thies, D., Schweigert, G., Mutterlose, J., Geologie, I., Hannover, L., 2019. Evaluation of shark tooth diagenesis-screening methods and the application of their stable oxygen isotope data for palaeoenvironmental reconstructions. J. Geol. Soc. Lond. 176, 482–491.
- Iacumin, P., Bocherens, H., Mariotti, A., Longinelli, A., 1996. Oxygen isotope analyses of co-existing carbonate and phosphate in biogenic apatite: a way to monitor diagenetic alteration of bone phosphate? Earth Planet. Sci. Lett. 142, 1–6.
- Jambura, P.L., Pfaff, C., Underwood, C.J., Ward, D.J., Kriwet, J., 2018. Tooth mineralization and histology patterns in extinct and extant snaggletooth sharks, hemipristis (carcharhiniformes, hemigaleidae)—evolutionary significance or ecological adaptation? PLoS One 13, 1–21. https://doi.org/10.1371/journal. pone.0200951.
- Jambura, P.L., Kindlimann, R., López-Romero, F., Marramà, G., Pfaff, C., Stumpf, S., Türtscher, J., Underwood, C.J., Ward, D.J., Kriwet, J., 2019. Micro-computed tomography imaging reveals the development of a unique tooth mineralization pattern in mackerel sharks (Chondrichthyes; Lamniformes) in deep time. Sci. Rep. 9, 1–13. https://doi.org/10.1038/s41598-019-46081-3.
- Jenkyns, H.C., 2010. Geochemistry of oceanic anoxic events. Geochem. Geophys. Geosyst. 11, 1–30. https://doi.org/10.1029/2009GC002788.
- Kast, E.R., Griffiths, M.L., Kim, S.L., Rao, Z.C., Shimada, K., Becker, M.A., Maisch, H.M., Eagle, R.A., Clarke, C.A., Neumann, A.N., Karnes, M.E., Lüdecke, T., Leichliter, J.N., Martinez-Garcia, A., Akhtar, A.A., Wang, X.T., Haug, G.H., Sigman, D.M., 2022. Cenozoic megatooth sharks occupied extremely high trophic positions. Sci. Adv. 6529, 7–18.
- Keenan, S.W., 2016. From bone to fossil: a review of the diagenesis of bioapatite. Am. Mineral. 101, 1943–1951. https://doi.org/10.2138/am-2016-5737.
- Khozyem, H., Adatte, T., Keller, G., Spangenberg, J.E., 2021. Organic carbon isotope records of the Paleocene- Eocene thermal maximum event in India provide new insights into mammal origination and migration. J. Asian Earth Sci. 212 https://doi. org/10.1016/j.jseaes.2021.104736.
- Kiel, S., Jakubowicz, M., Altamirano, A., Belka, Z., Dopieralska, J., Urbina, M., Salas-Gismondi, R., 2023. The late Cenozoic evolution of the Humboldt Current System in coastal Peru: Insights from neodymium isotopes. Gondwana Res. 116, 104–112. https://doi.org/10.1016/j.gr.2022.12.008.
- Kim, S.L., Casper, D.R., Galván-Magaña, F., Ochoa-Díaz, R., Hernández-Aguilar, S.B., Koch, P.L., 2012a. Carbon and nitrogen discrimination factors for elasmobranch soft tissues based on a long-term controlled feeding study. Environ. Biol. Fish 95, 37–52. https://doi.org/10.1007/s10641-011-9919-7.
- Kim, S.L., Del Rio, C.M., Casper, D., Koch, P.L., 2012b. Isotopic incorporation rates for shark tissues from a long-Term captive feeding study. J. Exp. Biol. 215, 2495–2500. https://doi.org/10.1242/jeb.070656.
- Kim, S.L., Eberle, J.J., Bell, D.M., Fox, D.A., Padilla, A., 2014. Evidence from shark teeth for a brackish Arctic Ocean in the Eocene greenhouse evidence from shark teeth for a brackish Arctic Ocean in the Eocene. Geology. https://doi.org/10.1130/G35675.1.
- Kim, S.L., Zeichner, S.S., Colman, A.S., Scher, H.D., Kriwet, J., Mörs, T., Huber, M., 2020. Probing the Ecology and climate of the Eocene Southern Ocean with Sand Tiger Sharks Striatolamia macrota. Paleoceanogr. Paleoclimatol. 35, 1–21. https://doi. org/10.1029/2020PA003997.
- Kneebone, J., Chisholm, J., Skomal, G.B., 2012. Seasonal residency, habitat use, and site fidelity of juvenile sand tiger sharks Carcharias taurus in a Massachusetts estuary. Mar. Ecol. Prog. Ser. 471, 165–181. https://doi.org/10.3354/meps09989.
- Kneebone, J., Chisholm, J., Skomal, G., 2014. Movement patterns of juvenile sand tigers (Carcharias taurus) along the east coast of the USA. Mar. Biol. 161, 1149–1163. https://doi.org/10.1007/s00227-014-2407-9.
- Kocsis, L., Vennemann, T.W., Fontignie, D., 2007. Migration of sharks into freshwater systems during the Miocene and implications for Alpine paleoelevation. Geology 35, 451–454. https://doi.org/10.1130/G23404A.1.
- Kocsis, L., Vennemann, T.W., Fontignie, D., Baumgartner, C., Montanari, A., Jelen, B., 2008. Oceanographic and climatic evolution of the Miocene Mediterranean deduced

- from Nd, Sr, C, and O isotope compositions of marine fossils and sediments. Paleoceanography 23. https://doi.org/10.1029/2007PA001540.
- Kocsis, L., Gheerbrant, E., Mouflih, M., Cappetta, H., Yans, J., Amaghzaz, M., 2014. Comprehensive stable isotope investigation of marine biogenic apatite from the late Cretaceous-early Eocene phosphate series of Morocco. Palaeogeogr. Palaeoclimatol. Palaeoecol. 394, 74–88. https://doi.org/10.1016/j.palaeo.2013.11.002.
- Kocsis, L., Vennemann, T.W., Ulianov, A., Brunnschweiler, J.M., 2015. Characterizing the bull shark Carcharhinus leucas habitat in Fiji by the chemical and isotopic compositions of their teeth. Environ. Biol. Fish 98, 1609–1622. https://doi.org/ 10.1007/s10641-015-0386-4.
- Kohn, M.J., Cerling, T.E., 2002. Stable isotope compositions of biological apatite. Phosphates Geochemical. Geobiol. Mater. Import. 48, 455–488. https://doi.org/ 10.2138/rmg.2002.48.12.
- Kolodny, Y., Luz, B., 1992. The isotopic record of oxygen in phosphates of fossil fish -Devonian to recent. Paleontol. Soc. Spec. Publ. 105–119 https://doi.org/10.1017/ s2475262200007310
- Kolodny, Y., Luz, B., Navon, O., 1983. Oxygen isotope variations in phosphate of biogenic apatites, I. Fish bone apatite-rechecking the rules of the game. Earth Planet. Sci. Lett. 64, 398–404. https://doi.org/10.1016/0012-821X(83)90100-0.
- Lécuyer, C., Grandjean, P., Emig, C.C., 1996. Determination of oxygen isotope fractionation between water and phosphate from living lingulids: potential application to palaeoenvironmental studies. Palaeogeogr. Palaeoclimatol. Palaeoecol. 126, 101–108.
- Lecuyer, C., Balter, V., Martineau, F., Fourel, F., Bernard, A., Amiot, R., Gardien, V., Otero, O., Legendre, S., Panczer, G., Simon, L., Martini, R., 2010. Oxygen isotope fractionation between apatite-bound carbonate and water determined from controlled experiments with synthetic apatites precipitated at 10–37 ° C. Geochim. Cosmochim. Acta 74, 2072–2081. https://doi.org/10.1016/j.gca.2009.12.024.
- Lécuyer, C., Amiot, R., Touzeau, A., Trotter, J., 2013. Calibration of the phosphate δ 18 O thermometer with carbonate – water oxygen isotope fractionation equations. Chem. Geol. 347, 217–226. https://doi.org/10.1016/j.chemgeo.2013.03.008.
- Lee-Thorp, J., 2002. Two decades of progress towards understanding fossilization processes and isotopic signals in calcified tissue minerals. Archaeometry 44, 435–446. https://doi.org/10.1111/1475-4754.t01-1-00076.
- Leichliter, J.N., Lüdecke, T., Foreman, A.D., Duprey, N.N., Winkler, D.E., Kast, E.R., Vonhof, H., Sigman, D.M., Haug, G.H., Clauss, M., Tütken, T., Martínez-García, A., 2021. Nitrogen isotopes in tooth enamel record diet and trophic level enrichment: results from a controlled feeding experiment. Chem. Geol. 563 https://doi.org/10.1016/j.chemgeo.2020.120047.
- Leuzinger, L., Kocsis, L., Luz, Z., Vennemann, T., Ulyanov, A., Fernández, M., 2023. Latest Maastrichtian middle- and high-latitude mosasaurs and fish isotopic composition: carbon source, thermoregulation strategy, and thermal latitudinal gradient. Paleobiology 49, 353–373. https://doi.org/10.1017/pab.2022.38.
- Longinelli, A., 1984. Oxygen isotopes in mammal bone phosphate: a new tool for paleohydrological and paleoclimatological research? Geochim. Cosmochim. Acta 48, 385–390.
- Longinelli, A., Nuti, S., 1973. Oxygen isotope measurements of phosphate from fish teeth and bones. Earth Planet. Sci. Lett. 20, 337–340.
- Lu, Y., Papagerakis, P., Yamakoshi, Y., Hu, J.C.C., Bartlett, J.D., Simmer, J.P., 2008. Functions of KLK4 and MMP-20 in dental enamel formation. Biol. Chem. 389, 695–700. https://doi.org/10.1515/BC.2008.080.
- Luz, B., Kolodny, Y., 1985. Oxygen isotope variations in phosphate of biogenic apatites,IV. Mammal teeth and bones. Earth Planet. Sci. Lett. 75, 29–36.Maisey, J.G., 2012. What is an 'elasmobranch'? The impact of palaeontology in
- Maisey, J.G., 2012. What is an 'elasmobranch'? The impact of palaeontology in understanding elasmobranch phylogeny and evolution. J. Fish Biol. 80, 918–951. https://doi.org/10.1111/j.1095-8649.2012.03245.x.
- https://doi.org/10.1111/j.1095-8649.2012.03245.x.
  Martin, C., Bentaleb, I., Kaandorp, R., Iacumin, P., Chatri, K., 2008. Intra-tooth study of modern rhinoceros enamel δ 18 O is the difference between phosphate and carbonate δ 18 O a sound diagenetic test? Palaeogeogr. Palaeoclimatol. Palaeoecol. 266, 183–189. https://doi.org/10.1016/j.palaeo.2008.03.039.
- McConnaughey, T.A., Burdett, J., Whelan, J.F., Paull, C.K., 1997. Carbon isotopes in biological carbonates: Respiration and photosynthesis. Geochim. Cosmochim. Acta 61, 611–622. https://doi.org/10.1016/S0016-7037(96)00361-4.
- McCormack, J., Griffiths, M.L., Kim, S.L., Shimada, K., Karnes, M., Maisch, H., Pederzani, S., Bourgon, N., Jaouen, K., Becker, M.A., Jöns, N., Sisma-ventura, G., Straube, N., Pollerspöck, J., Hublin, J., 2022. Trophic position of Otodus megalodon and great white sharks through time revealed by zinc isotopes. Nat. Commun. 13, 1–10. https://doi.org/10.1038/s41467-022-30528-9.
- McCormack, J., Karnes, M., Haulsee, D., Fox, D., Kim, S.L., 2023. Shark teeth zinc isotope values document intrapopulation foraging differences related to ontogeny and sex. Commun. Biol. 6, 711. https://doi.org/10.1038/s42003-023-05085-6.
- Miake, Y., Aoba, T., Moreno, E.C., Shimoda, S., Prostak, K., Suga, S., 1991. Ultrastructural studies on crystal growth of enameloid minerals in elasmobranch and teleost fish. Calcif. Tissue Int. 48, 204–217. https://doi.org/10.1007/BF02570556.
- Mine, A.H., Waldeck, A., Olack, G., Hoerner, M.E., Alex, S., Colman, A.S., 2017. Microprecipitation and  $\delta$ 18O analysis of phosphate for paleoclimate and biogeochemistry research. Chem. Geol. 460, 1–14. https://doi.org/10.1016/j.chemgeo.2017.03.032.
- Moeller, I.J., Melsen, B., Jensen, S.J., Kirkegaard, E., 1975. A histological, chemical and X-ray diffraction study on contemporary (Carcharias glaucus) and fossilized (Macrota odontaspis) shark teeth. Arch. Oral Biol. 20 https://doi.org/10.1016/ 0003-9969(75)90056-4.
- Ounis, A., Kocsis, L., Chaabani, F., Pfeifer, H.R., 2008. Rare earth elements and stable isotope geochemistry (613C and 618O) of phosphorite deposits in the Gafsa Basin, Tunisia. Palaeogeogr. Palaeoclimatol. Palaeoecol. 268, 1–18. https://doi.org/10.1016/j.palaeo.2008.07.005.

- Passey, B.H., Cerling, T.E., 2002. Tooth enamel mineralization in ungulates:
  Implications for recovering a primary isotopic time-series. Geochim. Cosmochim. Acta 66, 3225–3234.
- Passey, B.H., Robinson, T.F., Ayliffe, L.K., Cerling, T.E., Sponheimer, M., Dearing, M.D., Roeder, B.L., Ehleringer, J.R., 2005. Carbon isotope fractionation between diet, breath CO2, and bioapatite in different mammals. J. Archaeol. Sci. 32, 1459–1470. https://doi.org/10.1016/j.jas.2005.03.015.
- Pellegrini, M., Lee-thorp, J.A., Donahue, R.E., 2011. Exploring the variation of the δ18Op and δ18Oc relationship in enamel increments. Palaeogeogr. Palaeoclimatol. Palaeoecol. 310, 71–83. https://doi.org/10.1016/j.palaeo.2011.02.023.
- Podlesak, D.W., Torregrossa, A., Ehleringer, J.R., Dearing, M.D., Passey, B.H., Cerling, T. E., 2008. Turnover of oxygen and hydrogen isotopes in the body water, CO2, hair, and enamel of a small mammal. Geochim. Cosmochim. Acta 72, 19–35. https://doi.org/10.1016/j.gca.2007.10.003.
- Polo-Silva, C.J., Galván-Magaña, F., Delgado-Huertas, A., 2012. Trophic inferences of blue shark (Prionace glauca) in the Mexican Pacific from stable isotope analysis in teeth. Rapid Commun. Mass Spectrom. 26, 1631–1638. https://doi.org/10.1002/ rcm.6275.
- Prokoph, A., Shields, G.A., Veizer, J., 2008. Compilation and time-series analysis of a marine carbonate δ180, δ13C, 87Sr/86Sr and δ34S database through Earth history. Earth-Sci. Rev. 87, 113–133. https://doi.org/10.1016/j.earscirev.2007.12.003.
- Pucéat, E., Joachimski, M.M., Bouilloux, A., Monna, F., Bonin, A., Motreuil, S., Morinière, P., Hénard, S., Mourin, J., Dera, G., Quesne, D., 2010. Revised phosphatewater fractionation equation reassessing paleotemperatures derived from biogenic apatite. Earth Planet. Sci. Lett. 298, 135–142. https://doi.org/10.1016/j. epsl.2010.07.034.
- Sharp, Z.D., 2017. Terminology, standards and mass spectrometry. In: Principles of Stable Isotope Geochemistry.
- Shiffman, D.S., Ajemian, M.J., Carrier, J.C., Daly-Engel, T.S., Davis, M.M., Dulvy, N.K., Grubbs, R.D., Hinojosa, N.A., Imhoff, J., Kolmann, M.A., Nash, C.S., Paig-Tran, E.W. M., Peele, E.E., Skubel, R.A., Wetherbee, B.M., Whitenack, L.B., Wyffels, J.T., 2020. Trends in chondrichthyan research: an analysis of three decades of conference abstracts. Copeia 108, 122–131. https://doi.org/10.1643/071-19-179R.
- Shipley, O.N., Henkes, G.A., Gelsleichter, J., Morgan, C.R., Schneider, E.V., Talwar, B.S., Frisk, M.G., 2021. Shark tooth collagen stable isotopes (615N and 613C) as ecological proxies. J. Anim. Ecol. 90, 2188–2201. https://doi.org/10.1111/1365-2656 13518
- Sire, J.Y., Davit-Béal, T., Delgado, S., Gu, X., 2007. The origin and evolution of enamel mineralization genes. Cells Tissues Organs 186, 25–48. https://doi.org/10.1159/ 000102679.
- Sisma-Ventura, G., Tutken, T., Peters, S.T.M., Bialik, O.M., Zohar, I., Pack, A., 2019. Past aquatic environments in the Levant inferred from stable isotope compositions of carbonate and phosphate in fish teeth. PLoS One 14, 1–18.
- Smith, M.M., Johanson, Z., Underwood, C., Diekwisch, T.G.H., 2012. Pattern formation in development of chondrichthyan dentitions: a review of an evolutionary model. Hist. Biol. Int. J. Paleobiol. 37–41 https://doi.org/10.1080/08912963.2012.662228.
- Suga, S., Taki, Y., Ogawa, M., Taki, Y., 1991. Fluoride and iron concentrations in the Enameloid of lower teleostean fish. Mech. Phylogen. Mineral. Biol. Syst. 439–446. https://doi.org/10.1177/00220345930720051301.
- Tagliabue, A., Bopp, L., 2008. Towards understanding global variability in ocean carbon-13. Glob. Biogeochem. 22, 1–13. https://doi.org/10.1029/2007GB003037. Teter, S.M., Wetherbee, B.M., Fox, D.A., Lam, C.H., Kiefer, D.A., Shivji, M., 2015.
- Teter, S.M., Wetnerbee, B.M., Fox, D.A., Lam, C.H., Klefer, D.A., Shiyl, M., 2015.
  Migratory patterns and habitat use of the sand tiger shark (Carcharias taurus) in the western North Atlantic. Mar. Freshw. Res. 66, 158–169. https://doi.org/10.1071/MF14129.
- Trayler, R.B., Kohn, M.J., 2017. Tooth enamel maturation reequilibrates oxygen isotope compositions and supports simple sampling methods. Geochim. Cosmochim. Acta 198, 32–47. https://doi.org/10.1016/j.gca.2016.10.023.
- Trayler, R.B., Landa, P.V., Kim, S.L., 2023. Evaluating the efficacy of collagen isolation using stable isotope analysis and infrared spectroscopy. J. Archaeol. Sci. 151, 1–9. https://doi.org/10.1016/j.jas.2023.105727.
- Trueman, C.N.G., Behrensmeyer, A.K., Tuross, N., Weiner, S., 2004. Mineralogical and compositional changes in bones exposed on soil surfaces in Amboseli National Park, Kenya: Diagenetic mechanisms and the role of sediment pore fluids. J. Archaeol. Sci. 31, 721–739. https://doi.org/10.1016/j.jas.2003.11.003.
- Van Baal, R.R., Janssen, R., van der Lubbe, H.J.L., Schulp, A.S., Jagt, J.W.M., Vonhof, H. B., 2013. Oxygen and carbon stable isotope records of marine vertebrates from the type Maastrichtian, the Netherlands and Northeast Belgium (late cretaceous). Palaeogeogr. Palaeoclimatol. Palaeoecol. 392, 71–78. https://doi.org/10.1016/j.palaeo.2013.08.020.
- Vennemann, T.W., Hegner, E., 1998. Oxygen, strontium, and neodymium isotope composition of fossil shark teeth as a proxy for the palaeoceanography and palaeoclimatology of the Miocene northern Alpine Paratethys. Palaeogeogr. Palaeoclimatol. Palaeoecol. 142, 107–121. https://doi.org/10.1016/S0031-0182 (98)00062-5.
- Vennemann, T.W., Hegner, E., Cliff, G., Benz, G.W., 2001. Isotopic composition of recent shark teeth as a proxy for environmental conditions. Geochim. Cosmochim. Acta 65, 1583–1599. https://doi.org/10.1016/S0016-7037(00)00629-3.
- Waddell, L.M., Moore, T.C., 2008. Salinity of the Eocene Arctic Ocean from oxygen isotope analysis of fish bone carbonate. Paleoceanography 23, 1–14. https://doi.org/ 10.1029/2007PA001451.
- Wang, K., Chatterton, B.D.E., Wang, Y., 1997. An organic carbon isotope record of late Ordovician to early Silurian marine sedimentary rocks, Yangtze Sea, South China: Implications for CO2 changes during the Hirnantian glaciation. Palaeogeogr. Palaeoclimatol. Palaeoecol. 132, 147–158. https://doi.org/10.1016/S0031-0182 (97)00046-1.

- Whitenack, L.B., Kim, S.L., Sibert, E.C., 2022. Bridging the Gap between Chondrichthyan Paleobiology and Biology. Biology of Sharks and Their Relatives.
- Zachos, J.C., Dickens, G.R., Zeebe, R.E., 2008. An early Cenozoic perspective on greenhouse warming and carbon-cycle dynamics. Nature 451, 279–283. https://doi. org/10.1038/nature06588.
- Zachos, J., Pagani, M., Sloan, L., Thomas, E., Billups, K., 2001. Trends, rhythms, and aberrations in global climate 65 Ma to present. science 292 (5517), 686–693. https://doi.org/10.1126/science.1059412.
- Zacke, A., Voigt, S., Joachimski, M.M., Gale, A.S., Ward, D.J., Tutken, T., 2009. Surface-water freshening and high-latitude river discharge in the Eocene. J. Geol. Soc. Lond. 166, 969–980. https://doi.org/10.1144/0016-76492008-068.Surface-water.
- Zazzo, A., Lécuyer, C., Mariotti, A., 2004a. Experimentally-controlled carbon and oxygen isotope exchange between bioapatites and water under inorganic and microbially-
- mediated conditions. Geochim. Cosmochim. Acta 68, 1–12. https://doi.org/ 10.1016/S0016-7037(03)00278-3.
- Zazzo, A., Lecuyer, C., Sheppard, S.M.F., Grandjean, P., Mariotti, A., 2004b. Diagenesis and the reconstruction of paleoenvironments: a method to restore original d18 O values of carbonate and phosphate from fossil tooth enamel. Geochim. Cosmochim. Acta 68, 2245–2258. https://doi.org/10.1016/j.gca.2003.11.009.
- Zeebe, R.E., 2007. An expression for the overall oxygen isotope fractionation between the sum of dissolved inorganic carbon and water. Geosyst. Geochem. Geophys. 8 https://doi.org/10.1029/2007GC001663.
- Zeichner, S.S., Colman, A.S., Koch, P.L., Polo-Silva, C., Galván-Magaña, F., Kim, S.L., 2017. Discrimination factors and incorporation rates for organic matrix in shark teeth based on a captive feeding study. Physiol. Biochem. Zool. 90, 257–272. https://doi.org/10.1086/689192.